

1 **Polar dimethylsulfide (DMS) production insensitive to ocean**
2 **acidification during shipboard microcosm experiments: a**
3 **meta-analysis of 18 experiments from temperate to polar**
4 **waters.**

5 Frances E. Hopkins¹, Philip D. Nightingale¹, John A. Stephens¹, C. Mark Moore², Sophie
6 Richier², Gemma L. Cripps², Stephen D. Archer³

7 ¹Plymouth Marine Laboratory, Plymouth, PL1 3DH, U.K.

8 ²Ocean and Earth Science, National Oceanography Centre, University of Southampton,
9 Southampton, U.K.

10 ³Bigelow Laboratory for Ocean Sciences, Maine, U.S.A.

11 *Correspondence to:* Frances E. Hopkins (fhop@pml.ac.uk)

12 **Abstract.** Emissions of dimethylsulfide (DMS) from the polar oceans play a key role in
13 atmospheric processes and climate. Therefore, it is important to increase our understanding of
14 how DMS production in these regions may respond to climate change. The polar oceans are
15 particularly vulnerable to ocean acidification (OA). However, our understanding of the polar
16 DMS response is limited to two studies conducted in Arctic waters, where in both cases DMS
17 concentrations decreased with increasing acidity. Here, we report on our findings from seven
18 summertime shipboard microcosm experiments undertaken in a variety of locations in the
19 Arctic Ocean and Southern Ocean. These experiments reveal no significant effects of short
20 term OA on the net production of DMS by planktonic communities. This is in contrast to
21 similar experiments from temperate NW European shelf waters where surface ocean
22 communities responded to OA with significant increases in dissolved DMS concentrations. A
23 meta-analysis of the findings from both temperate and polar waters ($n = 18$ experiments)
24 reveals clear regional differences in the DMS response to OA. Based on our findings, we
25 hypothesise that the differences in DMS response between temperate and polar waters reflect
26 the natural variability in carbonate chemistry to which the respective communities of each
27 region may already be adapted. If so, future temperate oceans could be more sensitive to OA

28 resulting in a change in DMS emissions to the atmosphere, whilst perhaps surprisingly DMS
29 emissions from the polar oceans may remain relatively unchanged. By demonstrating that
30 DMS emissions from geographically distinct regions may vary in their response to OA, our
31 results may facilitate a better understanding of Earth's future climate. Our study suggests that
32 the way in which processes that generate DMS respond to OA may be regionally distinct and
33 this should be taken into account in predicting future DMS emissions and their influence on
34 Earth's climate.

35 **1 Introduction**

36 The trace gas dimethylsulfide (DMS) is a key ingredient in a cocktail of gases that exchange
37 between the ocean and atmosphere. Dissolved DMS is produced via the enzymatic
38 breakdown of dimethylsulfoniopropionate (DMSP), a secondary algal metabolite implicated
39 in a number of cellular roles, including the regulation of carbon and sulfur metabolism via an
40 overflow mechanism (Stefels, 2000) and protection against oxidative stress (Sunda et al.,
41 2002). Oceanic DMS emissions amount to 17 - 34 Tg S y⁻¹, representing 80 - 90% of all
42 marine biogenic S emissions, and up to 50% of global biogenic emissions (Lana et al., 2011).
43 DMS and its oxidation products play vital roles in atmospheric chemistry and climate
44 processes. These processes include aerosol formation pathways that influence the
45 concentration of cloud condensation nuclei (CCN) with implications for Earth's albedo and
46 climate (Charlson et al., 1987; Korhonen et al., 2008a), and the atmospheric oxidation
47 pathways of other key climate gases, including isoprene, ammonia and organohalogens (Chen
48 and Jang, 2012; von Glasow and Crutzen, 2004; Johnson and Bell, 2008). Thus, our ability to
49 predict the climate into the future requires an understanding of how marine DMS production
50 may respond to global change (Carpenter et al., 2012; Woodhouse et al., 2013; Menzo et al.,
51 2018).

52 The biologically-rich seas surrounding the Arctic pack ice are a strong source of DMS to the
53 Arctic atmosphere (Levasseur, 2013). A seasonal cycle in CCN numbers can be related to
54 seasonality in the Arctic DMS flux (Chang et al., 2011). Indeed, observations confirm that
55 DMS oxidation products promote the growth of particles to produce aerosols that may
56 influence cloud processes and atmospheric albedo (Bigg and Leck, 2001; Rempillo et al.,
57 2011; Korhonen et al., 2008b; Chang et al., 2011). Arctic new particle formation events and
58 peaks in aerosol optical depth (AOD) occur during summertime clean air periods (when
59 levels of anthropogenic black carbon diminish), and have been linked to chlorophyll *a*
60 maxima in surface waters and the presence of aerosols formed from DMS oxidation products
61 such as methanesulfonate (MSA). The atmospheric oxidation products of DMS - SO₂ and
62 H₂SO₄ - contribute to both the growth of existing particles and new particle formation (NPF)
63 in the Arctic atmosphere (Leaitch et al., 2013; Gabric et al., 2014; Sharma et al., 2012). Thus,
64 the ongoing and projected rapid loss of seasonal Arctic sea ice may influence the Arctic
65 radiation budget via changes to both the DMS flux and the associated formation and growth
66 of cloud-influencing particles (Sharma et al., 2012).

67 During its short but highly productive summer season, the Southern Ocean is a hotspot of
68 DMS flux to the atmosphere, influenced by the prevalence of intense blooms of DMSP-rich
69 *Phaeocystis antarctica* (Schoemann et al., 2005) and the presence of persistent high winds
70 particularly in regions north of the sub-Antarctic front (Jarníková and Tortell, 2016). Around
71 3.4 Tg of sulfur is released from the Southern Ocean to the atmosphere between December
72 and February, a flux that represents ~15 % of global annual emissions of DMS (Jarníková
73 and Tortell, 2016). Elevated CCN numbers are seen in the most biologically active regions of
74 the Southern Ocean, with a significant contribution from DMS-driven secondary aerosol
75 formation processes (McCoy et al., 2015; Korhonen et al., 2008a). DMS-derived aerosols
76 from this region are estimated to contribute 6 to 10 W m⁻² to reflected short wavelength

77 radiation, similar to the influence of anthropogenic aerosols in the polluted Northern
78 Hemisphere (McCoy et al., 2015). Given this important influence of polar DMS emissions on
79 atmospheric processes and climate, it is vital we increase our understanding of the influence
80 of future ocean acidification on DMS production.

81 The polar oceans are characterised by high dissolved inorganic carbon (C_T) concentrations
82 and a low carbonate system buffering capacity, mainly due to the increased solubility of CO_2
83 in cold waters (Sabine et al., 2004; Orr et al., 2005). This makes these regions particularly
84 susceptible to the impacts of ocean acidification (OA). For example, extensive carbonate
85 mineral undersaturation is expected to occur in Arctic waters within the next 20 – 80 years
86 (McNeil and Matear, 2008; Steinacher et al., 2009). OA has already led to a 0.1 unit decrease
87 in global surface ocean pH, with a further fall of ~ 0.4 units expected by the end of the century
88 (Orr et al., 2005). The greatest declines in pH are likely in the Arctic Ocean with a predicted
89 fall of 0.45 units by 2100 (Steinacher et al., 2009), with a fall of ~ 0.3 units predicted for the
90 Southern Ocean (McNeil and Matear, 2008; Hauri et al., 2016). OA is occurring at a rate not
91 seen on Earth for 300 Ma, and so the potential effects on marine organisms, communities and
92 ecosystems could be wide-ranging and severe (Raven et al., 2005; Hönisch et al., 2012).

93 Despite the imminent threat to polar ecosystems and the importance of DMS emissions to
94 atmospheric processes, our knowledge of the response of polar DMS production to OA is
95 limited to a single mesocosm experiment performed in a coastal fjord in Svalbard (Riebesell
96 et al., 2013; Archer et al., 2013) and one shipboard microcosm experiment with seawater
97 collected from Baffin Bay (Hussherr et al., 2017). Both studies reported significant
98 reductions in DMS concentrations with increasing levels of $p\text{CO}_2$ during seasonal
99 phytoplankton blooms. Hussherr et al. (2017) also saw reductions in total DMSP whilst
100 Archer et al. (2013) observed a significant increase in this compound, driven by CO_2 -induced

101 increases in growth and abundance of dinoflagellates. However, these two single studies
102 provide limited information on the wider response of the open Arctic or Southern Oceans.

103 Mesocosm experiments have been a critical tool for assessing OA effects on surface ocean
104 communities (Engel et al., 2005; Engel et al., 2008; Schulz et al., 2008; Hopkins et al., 2010;
105 Schulz et al., 2013; Webb et al., 2015; Kim et al., 2006; Kim et al., 2010; Crawford et al.,
106 2016; Webb et al., 2016). The response of DMS to OA has been examined several times,
107 predominantly at the same site in Norwegian coastal waters (Vogt et al., 2008; Hopkins et al.,
108 2010; Webb et al., 2015; Avgoustidi et al., 2012), twice in Korean coastal waters (Kim et al.,
109 2010; Park et al., 2014), and a single study in the coastal Arctic waters of Svalbard (Archer et
110 al., 2013). Mesocosm enclosures, ranging in volume from ~11,000 – 50,000 L, allow the
111 response of surface ocean communities to a range of CO₂ treatments to be monitored under
112 near-natural light and temperature conditions over time scales (weeks - months) that allow a
113 ‘winners vs loser’ dynamic to develop. The response of DMS cycling to elevated CO₂ is
114 generally driven by changes to the microbial community structure (Brussaard et al., 2013;
115 Archer et al., 2013; Hopkins et al., 2010; Engel et al., 2008). The size, construction and
116 associated costs of mesocosms has limited their deployment to coastal/sheltered waters,
117 resulting in minimal geographical coverage, and leaving large gaps in our understanding of
118 the response of open ocean phytoplankton communities to OA.

119 Here, we adopt an alternative but complementary approach to explore the effects of OA on
120 the cycling of DMS with the use of short-term shipboard microcosm experiments. We build
121 on the previous temperate NW European shelf studies of Hopkins & Archer (2014) by
122 presenting data from four previously unpublished experiments from the NW European shelf
123 cruise, and by extending our experimental approach to the Arctic and Southern Oceans.

124 Vessel-based research enables multiple short term (days) near-identical incubations to be
125 performed over extensive spatial scales, that encompass natural gradients in carbonate

126 chemistry, temperature and nutrients (Richier et al., 2014; Richier et al., 2018). This allows
127 an assessment to be made of how a range of surface ocean communities, adapted to a variety
128 of environmental conditions, respond to the same driver. The focus is then on the effect of
129 short-term CO₂ exposure on physiological processes, as well as the extent of the variability in
130 acclimation between communities. The capacity of organisms to acclimate to changing
131 environmental conditions contributes to the resilience of key ecosystem functions, such as
132 DMS production. Therefore, do spatially-diverse communities respond differently to short
133 term OA, and can this be explained by the range of environmental conditions to which each is
134 presumably already adapted? The rapid CO₂ changes implemented in this study, and during
135 mesocosm studies, are far from representative of the predicted rate of change to seawater
136 chemistry over the coming decades. Nevertheless, our approach can provide insight into the
137 physiological response and level of sensitivity to future OA of a variety of polar surface
138 ocean communities adapted to different in situ carbonate chemistry environments (Stillman
139 and Paganini, 2015), alongside the implications this may have for DMS production.

140 Communities of the NW European shelf consistently responded to acute OA with significant
141 increases in net DMS production, likely a result of an increase in stress-induced algal
142 processes (Hopkins and Archer, 2014). Do polar phytoplankton communities, which are
143 potentially adapted to contrasting biogeochemical environments, respond in the same way?
144 By expanding our approach to encompass both polar oceans, we can assess regional contrasts
145 in response. To this end, we combine our findings for temperate waters with those for the
146 polar oceans into a meta-analysis to advance our understanding of the regional variability and
147 drivers in the DMS response to OA.

148 **2 Material and Methods**

149 **2.1 Sampling stations**

150 This study presents new data from two sets of field experiments carried out as a part of the
151 UK Ocean Acidification Research Programme (UKOA) aboard the RRS James Clark Ross in
152 the sub-Arctic and Arctic in June-July 2012 (JR271) and in the Southern Ocean in January-
153 February 2013 (JR274). Data are combined with the results from an earlier study on board the
154 RRS Discovery (D366) described in Hopkins & Archer (2014) performed in the temperate
155 waters of the NW European shelf. Additionally, four previously unpublished experiments
156 from D366 are also included (E02b, E04b, E05b, E06) as well as two temperate experiments
157 from JR271 (NS and IB) (see Table 1). In total, 18 incubations were performed; 11 in
158 temperate and sub-Arctic waters of the NW European shelf and North Atlantic, 3 in Arctic
159 waters and 4 in the Southern Ocean. Figure 1 shows the cruise tracks, surface concentrations
160 of DMS and total DMSP (DMSPt) at CTD sampling stations as well as the locations of
161 sampling for shipboard microcosms (See Table 1 for further details).

162 **2.2 Shipboard microcosm experiments**

163 The general design and implementation of the experimental microcosms for JR271 and
164 JR274 was essentially the same as for D366 and described in Richier et al. (2014), (2018) and
165 Hopkins & Archer (2014), but with the additional adoption of trace metal clean sampling and
166 incubation techniques in the low trace metal open ocean waters (see Richier et al. (2018)). At
167 each station, pre-dawn vertical profiles of temperature, salinity, oxygen, fluorescence,
168 turbidity and irradiance were used to choose and characterise the depth of experimental water
169 collection. Subsequently, water was collected within the mixed layer from three successive
170 separate casts of a trace-metal clean titanium CTD rosette comprising twenty-four 10 L
171 Niskin bottles. Depth profiles of auxiliary measurements are shown in Figure 2. Each cast
172 was used to fill one of a triplicated set of experimental bottles (locations and sample depths,
173 Table 1). Bottles were sampled within a class-100 filtered air environment within a trace
174 metal clean container to avoid contamination during the set up. The water was directly

175 transferred into acid-cleaned 4.5 L polycarbonate bottles using acid-cleaned silicon tubing,
176 with no screening or filtration.

177 The carbonate chemistry within the experimental bottles was manipulated by addition of
178 equimolar HCl and NaHCO_3^- (1 mol L^{-1}) to achieve a range of CO_2 treatments: Mid CO_2
179 (Target: $550 \mu\text{atm}$), High CO_2 (Target: $750 \mu\text{atm}$), High+ CO_2 (Target: $1000 \mu\text{atm}$) and
180 High++ CO_2 (Target: $2000 \mu\text{atm}$) (Gattuso et al., 2010). Three treatment levels were used
181 during the sub-Arctic/Arctic microcosms (Mid, High, High+). For Southern Ocean
182 experiments, two experiments (*Drake Passage* and *Weddell Sea*) underwent combined CO_2
183 and Fe additions (ambient, Fe (2 nM), High CO_2 , Fe (2 nM) & High CO_2 (only high CO_2
184 treatments will be examined here; no response to Fe was detected in DMS or DMSP
185 concentrations). Three CO_2 treatments (High, High+, High++) were tested in the last two
186 experiments (*South Georgia* and *South Sandwich*). Full details of the carbonate chemistry
187 manipulations can be found in Richier et al. (2014) and Richier et al. (2018). Broadly,
188 achieved $p\text{CO}_2$ levels were well-matched to target values at the start of the experiments (0 h),
189 although differences in $p\text{CO}_2$ between target and initial values were greater in the higher
190 $p\text{CO}_2$ treatments, due to lowered carbonate system buffer capacity at higher $p\text{CO}_2$. For all 18
191 experiments, actual $p\text{CO}_2$ values at 0 h were on average around $89\% \pm 12\%$ ($\pm 1 \text{ SD}$) of
192 target values. The attained $p\text{CO}_2$ values, and $p\text{CO}_2$ at each experimental time point, are
193 presented in Figures 3 and 4. After first ensuring the absence of bubbles or headspace, the
194 bottles were sealed with high density polyethylene (HDPE) lids with silicone/
195 polytetrafluoroethylene (PTFE) septa and placed in the incubation container. Bottles were
196 incubated inside a custom-designed temperature- and light-controlled shipping container, set
197 to match ($\pm < 1^\circ\text{C}$) the *in situ* water temperature at the time of water collection (shown in
198 Table 1) (see Richier et al. 2018). A constant light level ($100 \mu\text{E m}^{-2} \text{ s}^{-1}$) was provided by
199 daylight simulating LED panels (Powerpax, UK). The light period within the microcosms

200 was representative of *in situ* conditions. For the sub-Arctic/Arctic Ocean stations,
201 experimental bottles were subjected to continuous light representative of the 24 h daylight of
202 the Arctic summer. For Southern Ocean and all temperate water stations, an 18:6 light: dark
203 cycle was used. Each bottle belonged to a set of triplicates, and sacrificial sampling of bottles
204 was performed at two time points (see Table 1 for exact times). Use of three sets of triplicates
205 for each time point allowed for the sample requirements of the entire scientific party (3 x 3
206 bottles, x 2 time points (see Table 1 for specific times for each experiment), x 4 CO₂
207 treatments = 72 bottles in total). Experiments were run for between 4 and 7 days (96 h – 168
208 h) (15 out of 18 experiments), with initial sampling proceeded by two further time points. For
209 three temperate experiments (E02b, E04b, E05b, see Table 1) a shorter 2 day incubation was
210 performed, with a single sampling point at the end. For E06 (see Table 1) high time
211 frequency sampling was performed (0, 1, 4, 14, 24, 48, 72, 96 h) although only the data at 48
212 h and 96 h is considered in this analysis. Incubation times were extended for Southern Ocean
213 stations *Weddell Sea*, *South Georgia* and *South Sandwich* (see Table 1) as minimal CO₂
214 response, attributed to slower microbial metabolism at low water temperatures, was observed
215 for Arctic stations and the first Southern Ocean station *Drake Passage*. The magnitude of
216 response was not related to incubation times, and expected differences in net growth rates (2-
217 to 3-fold higher in temperate compared to polar waters (Eppley, 1972)) did not account for
218 the differences in response magnitude despite the increased incubation time in polar waters
219 (see Richier et al. (2018) for detailed discussion). Samples for carbonate chemistry
220 measurements were taken first, followed by sampling for DMS, DMSP and related
221 parameters.

222 **2.3 Standing stocks of DMS and DMSP**

223 Methods for the determination of seawater concentrations of DMS and DMSP are identical to
224 those described in Hopkins & Archer (2014) and will therefore be described in brief here.
225 Seawater DMS concentrations were determined by cryogenic purge and trap, with gas
226 chromatography and pulsed flame photometric detection (GC-PFPD) (Archer et al., 2013).
227 DMSP concentrations were measured as DMS following alkaline hydrolysis. Samples for
228 total DMSP concentrations from temperate waters were fixed by addition of 35 μ l of 50 %
229 H₂SO₄ to 7 mL of seawater (Kiene and Slezak, 2006), and analysed following hydrolysis
230 within 2 months of collection (Archer et al., 2013). Samples of DMSP that were collected in
231 polar waters were hydrolysed within 1 h of sample collection and analysed 6 – 12 h later. The
232 H₂SO₄ fixation method was not used for samples from polar waters given the likely
233 occurrence of *Phaeocystis sp.* which can result in the overestimation of DMSP concentrations
234 (del Valle et al., 2009). Similarly, concentrations of DMSPp were determined at each time
235 point by gravity filtering 7 ml of sample onto a 25 mm GF/F filter and preserving the filter in
236 7 ml of 35 mM H₂SO₄ in MQ-water (temperate samples) or immediately hydrolysing (polar
237 samples) and analysing by GC-PFPD. DMS calibrations were performed using alkaline cold-
238 hydrolysis (1 M NaOH) of DMSP sequentially diluted three times in MilliQ water to give
239 working standards in the range 0.03 – 3.3 ng S mL⁻¹. Five point calibrations were performed
240 every 2 – 4 days throughout the cruise.

241 **2.4 *De novo* DMSP synthesis**

242 *De novo* DMSP synthesis and gross production rates were determined for all microcosm
243 experiments, except *Barents Sea* and *South Sandwich*, at each experimental time point, using
244 methods based on the approach of Stefels et al. (2009) and described in detail in Archer et al.
245 (2013) and Hopkins and Archer (2014). Triplicate rate measurements were determined for
246 each CO₂ level. For each rate measurement three x 500 mL polycarbonate bottles were filled

247 by gently siphoning water from each replicate microcosm bottle. Trace amounts of
 248 $\text{NaH}^{13}\text{CO}_3$, equivalent to ~6 % of *in situ* dissolved inorganic carbon (C_T), were added to each
 249 500 mL bottle. The bottles were incubated in the microcosm incubation container with
 250 temperature and light levels as described earlier. Samples were taken at 0 h, then at two
 251 further time points over a 6 - 9 h period. At each time point, 250 mL was gravity filtered in
 252 the dark through a 47 mm GF/F filter, the filter gently folded and placed in a 20 mL serum
 253 vial with 10 mL of Milli-Q and one NaOH pellet, and the vial was crimp-sealed. Samples
 254 were stored at -20°C until analysis by proton transfer reaction-mass spectrometer (PTR-MS)
 255 (Stefels et al. 2009).

256 The specific growth rate of DMSP (μDMSP) was calculated assuming exponential growth
 257 from:

$$258 \quad \mu_t(\Delta t^{-1}) = \alpha_k \times \text{AVG} \left[\ln \left(\frac{{}^{64}\text{MP}_{\text{eq}} - {}^{64}\text{MP}_{t-1}}{{}^{64}\text{MP}_{\text{eq}} - {}^{64}\text{MP}_t} \right), \ln \left(\frac{{}^{64}\text{MP}_{\text{eq}} - {}^{64}\text{MP}_t}{{}^{64}\text{MP}_{\text{eq}} - {}^{64}\text{MP}_{t+1}} \right) \right] \quad 1$$

259 (Stefels et al. 2009) where ${}^{64}\text{MP}_t$, ${}^{64}\text{MP}_{t-1}$, ${}^{64}\text{MP}_{t+1}$ are the proportion of $1 \times {}^{13}\text{C}$ labelled
 260 DMSP relative to total DMSP at time t , at the preceding time point ($t-1$) and at the subsequent
 261 time point ($t+1$), respectively. Values of ${}^{64}\text{MP}$ were calculated from the protonated masses of
 262 DMS as: $\text{mass } 64 / (\text{mass } 63 + \text{mass } 64 + \text{mass } 65)$, determined by PTR-MS. ${}^{64}\text{MP}_{\text{eq}}$ is the
 263 theoretical equilibrium proportion of $1 \times {}^{13}\text{C}$ based on a binomial distribution and the
 264 proportion of tracer addition. An isotope fractionation factor α_k of 1.06 is included, based on
 265 laboratory culture experiments using *Emiliana huxleyi* (Stefels et al. 2009). In vivo DMSP
 266 gross production rates during the incubations ($\text{nmol L}^{-1} \text{ h}^{-1}$) were calculated from μDMSP
 267 and the initial particulate DMSP (DMSP_p) concentration of the incubations (Hopkins &

268 Archer 2014, Stefels et al. 2009). These rates provide important information on how the
269 physiological status of DMSP-producing cells may be affected by OA within the bioassays.

270 **2.5 Seawater carbonate chemistry analysis**

271 The techniques and methods used to determine both the *in situ* and experimental carbonate
272 chemistry parameters, and to manipulate seawater carbonate chemistry within the
273 microcosms, are described in Richier et al. (2014) and will be only given in brief here.
274 Experimental T_0 measurements were taken directly from CTD bottles, and immediately
275 measured for total alkalinity (A_T) (Apollo SciTech AS-Alk2 Alkalinity Titrator) and
276 dissolved inorganic carbon (C_T) (Apollo SciTech C_T analyser (AS-C3) with LICOR 7000).
277 The CO2SYS programme (version 1.05) (Lewis and Wallace, 1998) was used to calculate the
278 remaining carbonate chemistry parameters including $p\text{CO}_2$.

279 Measurements of T_A and C_T were made from each bottle at each experimental time point and
280 again used to calculate the corresponding values for $p\text{CO}_2$ and pH_T . The carbonate chemistry
281 data for each sampling time point for each experiment are summarised in Supplementary
282 Table S1, S2 and S3 (Experimental starting conditions are given in Table 1).

283 **2.6 Chlorophyll a (Chl *a*) determinations**

284 Concentrations of Chl *a* were determined as described in Richier et al. (2014). Briefly, 100
285 mL aliquots of seawater from the incubation bottles were filtered through either 25 mm GF/F
286 (Whatman, 0.7 μm pore size) or polycarbonate filters (Whatman, 10 μm pore size) to yield
287 total and >10 μm size fractions, with the <10 μm fraction calculated by difference. Filters
288 were extracted in 6 mL HPLC-grade acetone (90%) overnight in a dark refrigerator.
289 Fluorescence was measured using a Turner Designs Trilogy fluorometer, which was regularly
290 calibrated with dilutions of pure Chl *a* (Sigma, UK) in acetone (90%).

291 **2.8 Community composition**

292 Small phytoplankton community composition was assessed by flow cytometry. For details of
293 methodology, see Richier et al. (2014).

294 **2.9 Data handling and statistical analyses**

295 Permutational analysis of variance (PERMANOVA) was used to analyse the difference in
296 response of DMS and DMSP concentrations to OA, both between and within the two polar
297 cruises in this study. Both dependant variables were analysed separately using a nested
298 factorial design with three factors; (i) Cruise Location: Arctic and Southern Ocean, (ii)
299 Experiment location nested within Cruise location (see Table 1 for station IDs) and (iii) CO₂
300 level: 385, 550, 750, 1000 and 2000 μ atm. Main effects and pairwise comparisons of the
301 different factors were analysed through unrestricted permutations of raw data. If a low
302 number of permutations were generated then the *p*-value was obtained through random
303 sampling of the asymptotic permutation distribution, using Monte Carlo tests.

304 One-way analysis of variance was used to identify differences in ratio of $>10 \mu$ m Chl *a* to
305 total Chl *a* ($chl_{>10\mu m} : chl_{tot}$, see Discussion). Initially, tests of normality were applied ($p < 0.05$
306 = not normal), and if data failed to fit the assumptions of the test, linearity transformations of
307 the data were performed (logarithmic or square root), and the ANOVA proceeded from this
308 point. The results of ANOVA are given as follows: *F* = ratio of mean squares, *df* = degrees of
309 freedom, *p* = level of confidence. For those data still failing to display normality following
310 transformation, a rank-based Kruskal-Wallis test was applied (*H* = test statistic, *df* = degrees
311 of freedom, *p* = level of confidence).

312 **3 Results**

313 **3.1 Sampling stations**

314 At temperate sampling stations, sea surface temperatures ranged from 10.7°C for *Iceland*
315 *Basin*, to 15.3°C for *Bay of Biscay*, with surface salinity in the range 34.1 – 35.2, with the
316 exception of station E05b which had a relatively low salinity of 30.5 (Figure 2 and Table 1).
317 Seawater temperatures at the polar microcosm sampling stations ranged from -1.5°C at sea-
318 ice influenced stations (*Greenland Ice-edge* and *Weddell Sea*) up to 6.5°C for *Barents Sea*
319 (Fig. 2 A). Salinity values at all the Southern Ocean stations were <34, whilst they were ~35
320 at all the Arctic stations with the exception of *Greenland Ice-edge* which had the lowest
321 salinity of 32.5 (Fig. 2 B). Phototrophic nanoflagellate abundances were variable, with >3 x
322 10⁴ cells mL⁻¹ at *Greenland Gyre*, 1.5 x 10⁴ cells mL⁻¹ at *Barents Sea* and <3 x 10³ cells mL⁻¹
323 for all other stations (Fig. 2 D). Total bacterial abundances ranged from 3 x 10⁵ cells mL⁻¹ at
324 *Greenland Ice-edge* up to 3 x 10⁶ cells mL⁻¹ at *Barents Sea* (Fig. 2 E).

325 Chl *a* concentrations in temperate waters ranged from 0.3 µg L⁻¹ for two North Sea stations
326 (*E05* and *North Sea*) up to 3.5 µg L⁻¹ for *Irish Sea* (Figure 2 and Table 1). Chl *a* was also
327 variable in polar waters, exceeding 4 µg L⁻¹ at *South Sandwich* and 2 µg L⁻¹ at *Greenland Ice-*
328 *edge*, whilst the remaining stations ranged from 0.2 µg L⁻¹ (*Weddell Sea*) to 1.5 µg L⁻¹
329 (*Barents Sea*) (Figure 2). The high Chl *a* concentrations at *South Sandwich* correspond to low
330 in-water irradiance levels at this station (Fig. 2 C).

331 In temperate waters, maximum DMS concentrations were generally seen in near surface
332 measurements, ranging from 1.0 nmol L⁻¹ for *E04* to 21.1 nmol L⁻¹ for *E06*, with rapidly
333 decreasing concentrations with depth (Figure 2 G). DMSP also generally peaked in the near
334 surface waters, ranging from 12.0 nmol L⁻¹ for *E04* to 72.5 nmol L⁻¹ for *E06*, but the
335 maximum overall DMSP concentration of 89.8 nmol L⁻¹ was observed at ~20 m for *E05b*
336 (Figure 2 H). Surface DMS concentrations in polar waters were generally lower than
337 temperate waters, ranging from 1 – 3 nmol L⁻¹, with the exception of *South Sandwich* where
338 concentrations of ~12 nmol L⁻¹ were observed (Figure 2 G). DMSP generally ranged from 12

339 – 20 nmol L⁻¹, except *Barents Sea* where surface concentrations exceeded 60 nmol L⁻¹
340 (Figure 2 H).

341 **3.2 Response of DMS and DMSP to OA**

342 The temporal trend in DMS concentrations showed a similar pattern for the three Arctic
343 Ocean experiments. Initial concentrations of 1 – 2 nmol L⁻¹ remained relatively constant over
344 the first 48 h and then showed small increases of 1 - 4 nmol L⁻¹ over the incubation period
345 (Figure 3). Increased variability between triplicate incubations became apparent in all three
346 Arctic experiments by 96 h, but no significant effects of elevated CO₂ on DMS
347 concentrations were observed. Initial DMSP concentrations were more variable, from 6 nmol
348 L⁻¹ at *Greenland Ice-edge* to 12 nmol L⁻¹ at *Barents Sea*, and either decreased slightly (net
349 loss 1 – 2 nmol L⁻¹ GG), or increased slightly (net increase ~4 nmol L⁻¹ *Greenland Ice-edge*,
350 ~3 nmol L⁻¹ *Barents Sea*) (Figure 5 A – C). DMSP concentrations were found to decrease
351 significantly in response to elevated CO₂ after 48 h for *Barents Sea* (Fig. 4 C, $t = 2.05$, $p =$
352 0.025), whilst no significant differences were seen after 96 h. No other significant responses
353 in DMSP were identified.

354 The range of initial DMS concentrations was greater at Southern Ocean sampling stations
355 compared to the Arctic, from 1 nmol L⁻¹ at *Drake Passage* up to 13 nmol L⁻¹ at *South*
356 *Sandwich* (Figure 4). DMS concentrations showed little change over the course of 96 – 168 h
357 incubations and no effect of elevated CO₂, with the exception of *South Sandwich* (Fig. 4 D).
358 Here, concentrations decreased sharply after 96 h by between 3 and 11 nmol L⁻¹.
359 Concentrations at 96 h were CO₂-treatment dependent, with significant decreases in DMS
360 concentration occurring with increasing levels of CO₂ (PERMANOVA, $t = 2.61$, $p = 0.028$).
361 Significant differences ceased to be detectable by the end of the incubations (168 h). Initial
362 DMSP concentrations were higher at the Southern Ocean stations than for Arctic stations,

363 ranging from 13 nmol L⁻¹ for *Weddell Sea* to 40 nmol L⁻¹ for *South Sandwich* (Figure 5 D –
364 G). Net increases in DMSP occurred throughout, except at South Georgia, and were on the
365 order of between <10 nmol L⁻¹ - >30 nmol L⁻¹ over the course of the incubations.

366 Concentrations were not generally pCO₂-treatment dependent with the exception of the final
367 time point at *South Georgia* (144 h) when a significantly lower DMSP with increasing CO₂
368 was observed (PERMANOVA, $t = -5.685$, $p < 0.001$).

369 Results from the previously unpublished experiments from temperate waters are in strong
370 agreement with the five experiments presented in Hopkins and Archer (2014), with
371 consistently decreased DMS concentrations and enhanced DMSP under elevated CO₂. The
372 data is presented in the Supplementary Information, Table S4 and Figure S2, and included in
373 the meta-analysis in section 4.1 of this paper.

374 **3.3 Response of de novo DMSP synthesis and production to OA**

375 Rates of *de novo* DMSP synthesis (μ DMSP) at initial time points ranged from 0.13 d⁻¹
376 (*Weddell Sea*, Fig. 6 G) to 0.23 d⁻¹ (*Greenland Ice-edge*, Fig. 6 C), whilst DMSP production
377 ranged from 0.4 nmol L⁻¹ d⁻¹ (*Greenland Gyre*, Fig. 6 B) to 2.27 nmol L⁻¹ d⁻¹ (*Drake Passage*,
378 Fig. 6 F). Maximum rates of μ DMSP of 0.37 -0.38 d⁻¹ were observed at *Greenland Ice-edge*
379 after 48 h of incubation in all CO₂ treatments (Fig. 6 C). The highest rates of DMSP
380 production were observed at *South Georgia* after 96 h of incubation, and ranged from 4.1 –
381 6.9 nmol L⁻¹ d⁻¹ across CO₂ treatments (Fig. 6 J). Rates of DMSP synthesis and production
382 were generally lower than those measured in temperate waters (Hopkins and Archer, 2014)
383 (Initial rates: μ DMSP 0.33 – 0.96 d⁻¹, 7.1 – 37.3 nmol L⁻¹ d⁻¹), but were comparable to
384 measurements made during an Arctic mesocosm experiment (Archer et al., 2013) (0.1 – 0.25
385 d⁻¹, 3 – 5 nmol L⁻¹ d⁻¹ in non-bloom conditions). The lower rates in cold polar waters likely
386 reflect slower metabolic processes and are reflected by standing stock DMSP concentrations

387 which were also lower than in temperate waters ($5 - 40 \text{ nmol L}^{-1}$ polar, $8 - 60 \text{ nmol L}^{-1}$
388 temperate (Hopkins and Archer, 2014)). No consistent of high CO_2 were observed for either
389 DMSP synthesis or production in polar waters, similar to findings for DMSP standing stocks.
390 However, some notable but contrasting differences between CO_2 treatments were observed.
391 There was a 36% and 37% increase in μDMSP and DMSP production respectively at 750
392 μatm for the *Drake Passage* after 96 h (Figure 6 E, F), and a 38% and 44% decrease in both
393 at 750 μatm after 144 h for *Weddell Sea* (Figure 5 G, H). For *Drake Passage*, the difference
394 between treatments at 96 h coincided with significantly higher nitrate concentrations in the
395 High CO_2 treatment (Nitrate/nitrite at 96 h: Ambient = $18.9 \pm 0.2 \mu\text{mol L}^{-1}$, $+\text{CO}_2 = 20.2 \pm$
396 $0.1 \mu\text{mol L}^{-1}$, ANOVA $F = 62.619$, $df = 1$, $p = 0.001$). However, it is uncertain whether the
397 difference in nutrient availability between treatments (approximately 5 %) would be
398 significant enough to strongly influence the rate of DMSP production.

399 The differences in DMSP production rates did not correspond to any other measured
400 parameter. It is possible that changes in phytoplankton community composition may have led
401 to differences in DMSP production rates for *Drake Passage* and *Weddell Sea*, but no
402 quantification of large cells (diatoms, dinoflagellates) was undertaken for these experiments.

403 **4 Discussion**

404 **4.1 Regional differences in the response of DMS(P) to OA**

405 We combine our findings from the polar oceans with those from temperate waters into a
406 meta-analysis in order to assess the regional variability and drivers in the DMS(P) response to
407 OA. Figures 7 and 8 provide an overview of the results discussed so far in this current study,
408 together with the results from Hopkins & Archer (2014) as well as the results from 4
409 previously unpublished microcosm experiments from the NW European shelf cruise and a
410 further 2 temperate water microcosm experiments from the Arctic cruise (*North Sea* and

411 *Iceland Basin*, Table 1). This gives a total of 18 microcosm experiments, each with between 1
412 and 3 high CO₂ treatments.

413 Hopkins & Archer (2014) reported consistent and significant increases in DMS concentration
414 in response to elevated CO₂ that were accompanied by significant decreases in DMSP
415 concentrations. Bacterially-mediated DMS processes appeared to be insensitive to OA, with
416 no detectable effects on dark rates of DMS consumption and gross production, and no
417 consistent response seen in bacterial abundance (Hopkins and Archer, 2014). In general,
418 there were large short-term decreases in Chl *a* concentrations and phototrophic nanoflagellate
419 abundance in response to elevated CO₂ in these experiments (Richier et al., 2014).

420 The relative treatment effects ($[x]_{\text{highCO}_2}/[x]_{\text{ambientCO}_2}$) for DMS and DMSP (Figure 7), DMSP
421 synthesis and production (Figure 8), and Chl *a* and phototrophic nanoflagellate abundance
422 (Figure 9) are plotted against the Revelle Factor of the sampled waters. The Revelle Factor
423 (R), calculated here with CO2Sys using measurements of carbonate chemistry parameters (R
424 = $(\Delta p\text{CO}_2/\Delta T\text{CO}_2)/(p\text{CO}_2/T\text{CO}_2)$, Lewis and Wallace, 1998), describes how the partial
425 pressure of CO₂ in seawater ($p\text{CO}_2$) changes for a given change in DIC (Sabine et al., 2004;
426 Revelle and Suess, 1957). Its magnitude varies latitudinally, with lower values (9 – 12) from
427 the tropics to temperate waters, and the highest values in cold high latitude waters (13 – 15).
428 Thus polar waters can be considered poorly buffered with respect to changes in DIC.

429 Therefore, biologically-driven seasonal changes in seawater $p\text{CO}_2$ would result in larger
430 changes in pH than would be experienced in temperate waters. (Egleston et al., 2010).

431 Furthermore, the seasonal sea ice cycle strongly influences carbonate chemistry, such that sea
432 ice regions exhibit wide fluctuations in carbonate chemistry (Revelle and Suess, 1957; Sabine
433 et al., 2004). Sampling stations with a R above ~12 represent the seven polar stations (right of
434 red dashed line Fig. 7, 8, 9). The surface waters of the polar oceans have naturally higher
435 levels of DIC and a reduced buffering capacity, driven by higher CO₂ solubility in colder

436 waters (Sabine et al., 2004). Thus, the relationship between experimental response and R is a
437 simple way of demonstrating the differences in response to OA between temperate and polar
438 waters and provides some insight into how the CO_2 sensitivity of different surface ocean
439 communities may relate to the *in situ* carbonate chemistry. The effect of elevated CO_2 on
440 DMS concentrations at polar stations, relative to ambient controls, was minimal at both
441 sampling points, and is in strong contrast to the results from experiments performed in waters
442 with lower values of R on the NW European shelf. In contrast, at temperate stations, DMSP
443 concentrations displayed a clear negative treatment effect, whilst at polar stations a positive
444 effect was evident under high CO_2 , and particularly at the first time point (48 – 96 h) (Fig. 7
445 C and D). *De novo* DMSP synthesis and DMSP production rates show a less consistent
446 response in either environment (Fig. 8 A and B), although a significant suppression of
447 DMSP production rates in temperate waters compared to polar waters was seen (Fig. 8 B,
448 Kruskal-Wallis One Way ANOVA $H = 8.711$, $df = 1$, $p = 0.003$). A similar but not significant
449 response was seen for *de novo* DMSP synthesis (Fig. 8A).

450 This data suggests that DMSP concentrations in polar waters may be upregulated in response
451 to OA compared to temperate waters. Given the potential photoprotective and antioxidant
452 role that DMSP plays, and which may be particularly relevant in the highly variable polar
453 sea-ice environment (e.g. irradiance, carbonate chemistry), these changes may reflect a
454 physiological protective response to the experimental OA (Sunda et al., 2002; Galindo et al.,
455 2016). An increase in DMSP concentrations could have either resulted from a physiological
456 up-regulation of DMSP synthesis or a reduction in bacterial DMSP consumption processes.
457 However, DMSP synthesis rates did not provide any conclusive evidence of upregulation in
458 polar waters. Instead, we observed a suppression of rates in temperate waters which may
459 reflect the adverse effects of rapid OA on DMSP producers (Richier et al. 2014, Hopkins and
460 Archer 2014). In contrast, the lesser response seen in polar waters may reflect a higher

461 acclimative tolerance to rapid changes in carbonate chemistry amongst polar communities.
462 Further experiments with polar communities would help to further unravel the potential
463 importance of such mechanisms, and whether they facilitated the ability of polar
464 phytoplankton communities to resist the high CO₂ treatments.

465 The responses to OA observed for DMS and DMSP production are likely to be reflected in
466 the dynamics of the DMSP-producing phytoplankton. In an assessment across all
467 experiments, Richier et al. (2018) showed that the maximal response to OA of total Chl *a* and
468 net growth rates of small phytoplankton (<10 μm) observed during each experiment,
469 declined the most in relation to increased buffering capacity and temperature of the initial
470 water. Generally, less significant relationships were found between the phytoplankton
471 response and the other wide range of physical, chemical or biological variables that were
472 examined (Richier et al. 2018).

473 In correspondence with the analyses carried out by Richier et al (2018), at 48 – 96 h (see
474 Table 1), a statistically significant difference in response was seen between temperate and
475 polar waters for Chl *a* (Kruskal-Wallis One Way ANOVA $H = 20.577$, $df = 1$, $p < 0.001$). In
476 general, at polar stations phytoplankton showed minimal response to elevated CO₂, in
477 contrast to a strong negative response in temperate waters (Fig. 9A). By the second time point
478 (96 – 144 h, see Table 1), no significant difference in response of Chl *a* between temperate
479 and polar waters was apparent (Fig. 9B). As shown in Richier et al. (2014), phototrophic
480 nanoflagellates responded to high CO₂ with large decreases in abundance in temperate waters
481 and increases in abundance in polar waters (Fig. 9 C and D), with some exceptions: *North*
482 *Sea* and *South Sandwich* gave the opposite response. The responses had lessened by the
483 second time point (96 – 168 h, see Table 1).

484 In contrast, bacterial abundance did not show the same regional differences in response to
485 high CO₂ (see Hopkins and Archer (2014) for temperate waters, and Figure S1,
486 supplementary information, for polar waters). Bacterial abundance in temperate waters gave
487 variable and inconsistent responses to high CO₂. For all Arctic stations, *Drake Passage* and
488 *Weddell Sea*, no response to high CO₂ was observed. For *South Georgia* and *South Sandwich*,
489 bacterial abundance increased at 1000 and 2000 µatm, with significant increases for *South*
490 *Georgia* after 144 h of incubation (ANOVA $F = 137.936$, $p < 0.001$). Additionally, at Arctic
491 stations *Greenland Gyre* and *Greenland Ice-edge*, no overall effect of increased CO₂ on rates
492 of DOC release, total carbon fixation or POC : DOC was observed (Poulton et al. 2016).

493 Overall, the observed differences in the regional response of DMSP and DMS to carbonate
494 chemistry manipulation could not be attributed to any other measured factor that varied
495 systematically between temperate and polar waters. These include ambient nutrient
496 concentrations, which varied considerably but where direct manipulation had no influence on
497 the response, and initial community structure, which was not a significant predictor of the
498 phytoplankton response (Richier et al. 2018).

499 **4.2 Influence of community cell-size composition on DMS response**

500 It has been proposed that variability in the concentrations of carbonate species (e.g. $p\text{CO}_2$,
501 HCO_3^- , CO_3^{2-}) experienced by phytoplankton is related to cell size, such that smaller-celled
502 taxa (<10 µm) with a reduced diffusive boundary layer are naturally exposed to relatively less
503 variability compared to larger cells (Flynn et al., 2012). Thus, short-term and rapid changes in
504 carbonate chemistry, such as the kind imposed during our microcosm experiments, may have
505 a disproportionate effect on the physiology and growth of smaller celled species. Larger cells
506 may be better able to cope with variability as normal cellular metabolism results in significant
507 cell surface changes in carbonate chemistry parameters (Richier et al., 2014). Indeed, the

508 marked response in DMS concentrations to short term OA in temperate waters has been
509 attributed to this enhanced sensitivity of small phytoplankton (Hopkins and Archer, 2014).
510 Was the lack of DMS response to OA in polar waters therefore a result of the target
511 communities being dominated by larger-celled, less carbonate-sensitive species?

512 Size-fractionated Chl *a* measurements give an indication of the relative contribution of large
513 and small phytoplankton cells to the community. For experiments in temperate waters, the
514 mean ratio of $>10 \mu\text{m}$ Chl *a* to total Chl *a* (hereafter $>10 \mu\text{m} : \text{total}$) of 0.32 ± 0.08 was lower
515 than the ratio for polar stations of 0.54 ± 0.13 (Table 2). Although the difference was not
516 statistically significant, this might imply a tendency towards communities dominated by
517 larger cells in the polar oceans, which may partially explain the apparent lack of DMS
518 response to elevated CO_2 . However, this is not a consistent explanation for the observed
519 responses. For example, the Arctic *Barents Sea* station had the lowest observed $>10 \mu\text{m} :$
520 *total* of 0.04 ± 0.01 , suggesting a community comprised almost entirely of $<10 \mu\text{m}$ cells; yet
521 the response to short term OA differed to the response seen in temperate waters. No
522 significant CO_2 effects on DMS or DMSP concentrations or production rates were observed
523 at this station, whilst total Chl *a* significantly increased under the highest CO_2 treatments
524 after 96 h (PERMANOVA $F = 33.239, p < 0.001$). Thus, our cell size theory does not hold for
525 all polar waters, suggesting that regardless of the dominant cell size, polar communities are
526 more resilient to OA. In the following section, we explore the causes of this apparent
527 insensitivity to OA in terms of the environmental conditions to which the communities have
528 presumably adapted.

529 **4.3 Adaptation to a variable carbonate chemistry environment**

530 Given that DMS production by polar phytoplankton communities appeared to be insensitive
531 to experimental OA compared to significant sensitivity in temperate communities, we

532 hypothesise that polar communities are adapted to greater natural variability in carbonate
533 chemistry over spatial and seasonal scales. The polar waters sampled during our study were
534 characterised by pronounced gradients in carbonate chemistry over small spatial scales, such
535 that surface ocean communities are more likely to have experienced fluctuations between
536 high pH and low pH over short time scales (Tynan et al., 2016). For example, in underway
537 samples taken along each cruise track, pH varied by 0.45 units (8.00 – 8.45) in the Arctic, and
538 0.40 units (8.30 - 7.90) in the Southern Ocean (Tynan et al. 2016). By comparison, pH varied
539 by 0.2 units (8.22 - 8.02) in underway samples from the NW European shelf sea cruise
540 (Rerolle et al. 2014).

541 The observed horizontal gradients in polar waters were driven by different physical and
542 biogeochemical processes in each ocean. In the Arctic Ocean, this variability in carbonate
543 chemistry was partly driven by physical processes that controlled water mass composition,
544 temperature and salinity, particularly in areas such as the Fram Strait and Greenland Sea. Along
545 the ice-edge and into the Barents Sea, biological processes exerted a strong control, as
546 abundant iron resulted in high chlorophyll concentrations, low DIC and elevated pH. By
547 contrast, variations in temperature and salinity had only a small influence on carbonate
548 chemistry in the Southern Ocean in areas with iron limitation, and larger changes were driven
549 by a combination of calcification, advection and upwelling. Where iron was replete, e.g. near
550 South Georgia, biological DIC drawdown had a large impact on carbonate chemistry (Tynan
551 et al. 2016). A further set of processes was in play in sea ice influenced regions. At the Arctic
552 ice edge, abundant iron drove strong bloom development along the ice edge, whilst sea ice
553 retreat in the Southern Ocean was not always accompanied by iron release (Tynan et al.
554 2016).

555 For comparison with Arctic stations, Hagens and Middelburg (2016) report a seasonal pH
556 variability of up to 0.25 units from a single site in the open ocean surface waters in the

557 Iceland Sea, whilst Kapsenberg et al. (2015) report an annual variability of 0.3 – 0.4 units in
558 the McMurdo Sound, Antarctica. This implies that both open ocean and sea ice-influenced
559 polar waters experience large variations in carbonate chemistry over seasonal cycles. By
560 contrast, monthly averaged surface $p\text{CO}_2$ data collected from station L4 in the Western
561 English Channel over the period 2007 – 2011 provides an example of typical carbonate
562 chemistry dynamics in NW European shelf sea waters. Over this period, pH had an annual
563 range of 0.15 units (8.05 – 8.20), accompanied by a range in $p\text{CO}_2$ of 302 – 412 μatm (Kitidis
564 et al., 2012).

565 The sea ice environment in particular is characterised by strong spatial and seasonal
566 variability in carbonate chemistry. Sea ice is inhabited by a specialised microbial community
567 with a complex set of metabolic and physiological adaptations allowing these organisms to
568 withstand wide fluctuations in pH up to as high as 9.9 in brine channels to as low as 7.5 in the
569 under-ice water (Thomas and Dieckmann, 2002; Rysgaard et al., 2012; Thoisen et al., 2015).

570 The open waters associated with the ice edge also experience strong gradients in pH and
571 other carbonate chemistry parameters. This can be attributed to two processes: 1. The strong
572 seasonal drawdown of DIC due to rapid biological uptake by phytoplankton blooms at the
573 productive ice edge which drives up pH. On the Arctic cruise, increases of up to 0.33 pH
574 units were attributed to such processes in this region (Tynan et al., 2016). The effect was less
575 dramatic in the Fe-limited and less productive Weddell Sea with gradients in pH ranging
576 from 8.20 – 8.10 (Tynan et al., 2016). 2. The drawdown of DIC is countered by the release
577 and accumulation of respired DIC under sea ice due to the degradation of organic matter.

578 However, this accumulation occurs in subsurface/bottom waters, which are isolated from the
579 productive surface mixed layer by strong physical stratification and hence, of less relevance
580 to the current study.

581 The influence of sea ice on carbonate chemistry combined with the strong biological
582 drawdown of DIC in polar waters may have influenced the ability of some of the
583 communities we sampled during our study to withstand the short term changes to carbonate
584 chemistry they experienced within the bioassays. Two of our sampling stations were ‘sea-ice
585 influenced’: *Greenland Ice Edge* and *Weddell Sea*. Both were in a state of sea ice retreat as
586 our sampling occurred in the summer months. Sampling for the *Greenland Ice Edge* station
587 was performed in open, deep water, near to an area of thick sea ice, with low fluorescence but
588 reasonable numbers of diatoms (Leakey, 2012). Similarly, the *Weddell Sea* station was
589 located near the edge of thick pack ice but in an area of open water that allowed sampling to
590 occur without hindrance by brash ice (Tarling, 2013). At both stations we saw little or no
591 response in DMS or DMSP to experimental acidification, which may imply that the *in situ*
592 communities were more or less adapted to fluctuations in pH. Our experimental OA resulted
593 in pH decreases of between 0.4 and 0.7 units. However, it is unclear whether the communities
594 we sampled were able to withstand the artificial pH perturbation because they were adapted
595 to living in sea ice, or whether they had adapted to cope with other fluctuations in carbonate
596 chemistry that occur in polar waters.

597 In summary, this demonstrates the high variability in carbonate chemistry, including pH,
598 which polar communities may experience relative to their temperate counterparts. This may
599 have resulted in adapted communities resilient to experimentally-induced OA. Of course, it is
600 important to recognise that this data represent only a snapshot (4 – 6 weeks) of a year, and
601 thus does not contain information on the range in variability over daily and seasonal cycles,
602 timescales which might be considered most important in terms of the carbonate system
603 variability experienced by the cells and how this drives CO₂ sensitivity (Flynn et al. 2012;
604 Richier et al. 2018). Nevertheless, this inherent carbonate chemistry variability experienced

605 by organisms living in polar waters may equip them with the resilience to cope with both
606 experimental and future OA.

607 Adaptation to such natural variability may induce the ability to resist abrupt changes within
608 the polar biological community (Kapsenberg et al., 2015). This is manifested here as
609 negligible impacts on rates of *de novo* DMSP synthesis and net DMS production. A number
610 of previous studies in polar waters have reported similar findings. Phytoplankton
611 communities were able to tolerate a $p\text{CO}_2$ range of 84 – 643 μatm in ~12 d minicosm
612 experiments (650 L) in Antarctic coastal waters, with no effects on nanophytoplankton
613 abundance, and enhanced abundance of picophytoplankton and prokaryotes (Davidson et al.,
614 2016; Thomson et al., 2016). In experiments under the Arctic ice, microbial communities
615 demonstrated the capacity to respond either by selection or physiological plasticity to
616 elevated CO_2 during short term experiments (Monier et al., 2014). Subarctic phytoplankton
617 populations demonstrated a high level of resilience to OA in short term experiments,
618 suggesting a high level of physiological plasticity that was attributed to the prevailing strong
619 gradients in $p\text{CO}_2$ levels experienced in the sample region (Hoppe et al., 2017). Furthermore,
620 a more recent study describing ten CO_2 manipulation experiments in Arctic waters found that
621 primary production was largely insensitive to OA over a large range of light and temperature
622 levels (Hoppe et al., 2018). This supports our hypothesis that, relative to temperate
623 communities, polar microbial communities may have a high capacity to compensate for
624 environmental variability (Hoppe et al., 2018), and are thus already adapted to, and are able
625 to tolerate, large variations in carbonate chemistry. Thus by performing multiple, replicated
626 experiments over a broad geographic range, the findings of this study imply that the DMS
627 response may be both a reflection of: (i) the level of sensitivity of the community to changes
628 in the mean state of carbonate chemistry, and (ii) the regional variability in carbonate
629 chemistry experienced by different communities. This highlights the limitations associated

630 with simple extrapolation of results from a small number of geographically-limited
631 experiments e.g. Six et al. (2013). Such an approach lacks a mechanistic understanding that
632 would allow a model to capture the regional variability in response that is apparent from the
633 microcosms experiments presented here.

634 **4.4 Comparison to an Arctic mesocosm experiment**

635 Experimental data clearly provide useful information on the potential future DMS response to
636 OA, but these data become most powerful when incorporated in Earth System Models (ESM)
637 to facilitate predictions of future climate. To date, two modelling studies have used ESM to
638 assess the potential climate feedback resulting from the DMS sensitivity to OA (Six et al.,
639 2013;Schwinger et al., 2017), and both have used results from mesocosm experiments.
640 However, the DMS responses to OA within our short term microcosm experiments contrast
641 with the results of most previous mesocosm experiments, and of particular relevance to this
642 study, an earlier Arctic mesocosm experiment (Archer et al., 2013). Whilst no response in
643 DMS concentrations to OA was generally seen in the polar microcosm experiments discussed
644 here, a significant decrease in DMS with increasing levels of CO₂ in the earlier mesocosm
645 study was seen. Therefore, it is useful to consider how the differences in experimental design,
646 and other factors, between microcosms and mesocosms may result in contrasting DMS
647 responses to OA.

648 The short duration of the microcosm experiments (4 – 7 d) allows the physiological
649 (phenotypic) capacity of the community to changes in carbonate chemistry to be assessed. In
650 other words, how well is the community adapted to variable carbonate chemistry and how
651 does this influence its ability to acclimate to change? Although the mesocosm experiment
652 considered a longer time period (4 weeks), the first few days can be compared to the
653 microcosms. No differences in DMS or DMSP concentrations were detected for the first
654 week of the mesocosm experiment, implying a certain level of insensitivity of DMS

655 production to the rapid changes in carbonate chemistry. In fact, when taking all previous
656 mesocosm experiments into consideration, differences in DMS concentrations have
657 consistently been undetectable during the first 5 – 10 days, implying there is a limited short-
658 term physiological response by the in situ communities (Hopkins et al., 2010; Avgoustidi et
659 al., 2012; Vogt et al., 2008; Kim et al., 2010; Park et al., 2014). This is in contrast to the
660 strong response in the temperate microcosms from the NW European shelf (Hopkins and
661 Archer, 2014). However, all earlier mesocosm experiments have been performed in coastal
662 waters, which like polar waters, can experience a large natural range in carbonate chemistry.
663 In the case of coastal waters this is driven to a large extent by the influence of riverine
664 discharge and biological activity (Fassbender et al., 2016). Thus coastal communities may
665 also possess a higher level of adaptation to variable carbonate chemistry compared to the
666 open ocean communities of the temperate microcosms (Fassbender et al., 2016).

667 The later stages of mesocosm experiments address a different set of hypotheses, and are less
668 comparable to the microcosms reported here. With time, an increase in number of generations
669 leads to community structure changes and taxonomic shifts, driven by selection on the
670 standing genetic variation in response to the altered conditions. Moreover, the coastal Arctic
671 mesocosms were enriched with nutrients after 10 days, affording relief from nutrient
672 limitation and allowing differences between $p\text{CO}_2$ treatments to be exposed, including a
673 strong DMS(P) response.(Archer et al., 2013; Schulz et al., 2013). During this period of
674 increased growth and productivity, CO_2 increases drove changes which reflected both the
675 physiological and genetic potential within the community, and resulted in taxonomic shifts.
676 The resultant population structure was changed, with an increase in abundance of
677 dinoflagellates, particularly *Heterocapsa rotundata*. Increases in DMSP concentrations and
678 DMSP synthesis rates were attributed to the population shift towards dinoflagellates. The
679 drivers of the reduced DMS concentrations were less clear, but may have been linked to

680 reduced DMSP-lyase capacity within the dominant phytoplankton, a reduction in bacterial
681 DMSP lysis, or an increase in bacterial DMS consumption rates (Archer et al., 2013). Again,
682 this is comparable to all other mesocosm experiments, wherein changes to DMS
683 concentrations can be associated with CO₂-driven shifts in community structure (Hopkins et
684 al., 2010; Avgoustidi et al., 2012; Vogt et al., 2008; Kim et al., 2010; Park et al., 2014; Webb
685 et al., 2015). However, given the lack of further experiments of a similar location, design and
686 duration to the Arctic mesocosm, it is unclear how representative the mesocosm result is of
687 the general community-driven response to OA in high latitude waters.

688 We did not generally see any broad-scale CO₂-effects on community structure in polar
689 waters. This can be demonstrated by a lack of significant differences in the mean ratio of >10
690 μm Chl *a* to total Chl *a* (>10 μm : total) between CO₂ treatments, implying there were no
691 broad changes in community composition (Table 2). *South Sandwich* was an exception to
692 this, where large and significant increases in the mean ratio of >10 μm : total were observed
693 at 750 μatm and 2000 μatm CO₂ relative to ambient CO₂ (ANOVA, $F = 207.144$, $p < 0.001$, df
694 = 3), demonstrated at even the short timescale of the microcosm experiments, it is possible
695 for some changes to community composition to occur. Interestingly, this was also the only
696 polar station that exhibited any significant effects on DMS after 96 h of incubation (Figure 4
697 D). However, given the lack of similar response at 1000 μatm, it remains equivocal whether
698 this was driven by a CO₂-effect or some other factor. The results of our microcosm
699 experiments suggest insensitivity of *de novo* DMSP production and net DMS production in
700 the microbial communities of the polar open oceans to short term changes in carbonate
701 chemistry. This may be driven by a high level of adaptation within the targeted
702 phytoplankton communities to naturally varying carbonate chemistry.

703 In contrast to our findings, a recent single 9 day microcosm experiment (Hussherr et al.,
704 2017) performed in Baffin Bay (Canadian Arctic) saw a linear 80% decrease in DMS
705 concentrations during spring bloom-like conditions. It should be noted that this response was
706 seen over a range of $p\text{CO}_2$ from 500 - 3000 μatm , far beyond the levels used in the present
707 study. Nevertheless, this implies that polar DMS production may be sensitive to OA at certain
708 times of the year, such as during the highly productive spring bloom, but less sensitive during
709 periods of low and stable productivity, such as the summer months sampled during this study.
710 Furthermore, a number of other studies from both the Arctic e.g. (Coello-Camba et al., 2014;
711 Holding et al., 2015; Thoisen et al., 2015) and the Southern Ocean e.g. (Trimborn et al.,
712 2017; Tortell et al., 2008; Hoppe et al., 2013) suggest that polar phytoplankton communities
713 can demonstrate sensitivity to OA, in contrast to our findings. This emphasises the need to
714 gain a more detailed understanding of both the spatial and seasonal variability in the polar
715 phytoplankton community and associated DMS response to changing ocean acidity.

716 **5 Conclusions**

717 We have shown that net DMS production by summertime polar open ocean microbial
718 communities is insensitive to OA during multiple, highly replicated short term microcosm
719 experiments. We provide evidence that, in contrast to temperate communities (Hopkins and
720 Archer, 2014), the polar communities we sampled were relatively insensitive to variations in
721 carbonate chemistry (Richier et al., 2018), manifested here as a minimal effect on net DMS
722 production. Our findings contrast with two previous studies performed in Arctic waters
723 (Archer et al. 2013; Hussherr et al. 2017) which showed significant decreases in DMS in
724 response to OA. These discrepancies may be driven by differences in experimental design,
725 variable sensitivity of microbial communities to changing carbonate chemistry between
726 different areas, or by variability in the response to OA depending on the time of year, nutrient
727 availability, and ambient levels of growth and productivity. This serves to highlight the

728 complex spatial and temporal variability in DMS response to OA which warrants further
729 investigation to improve model predictions.

730 Our results imply that the phytoplankton communities of the temperate microcosms initially
731 responded to the rapid increase in pCO₂ via a stress-induced response, resulting in large and
732 significant increases in DMS concentrations occurring over the shortest timescales (2 days),
733 with a lessening of the treatment effect with an increase in incubation time (Hopkins and
734 Archer 2014). The dominance of short response timescales in well-buffered temperate waters
735 may also indicate rapid acclimation of the phytoplankton populations following the initial
736 stress response, which forced the small-sized phytoplankton beyond their range of
737 acclimative tolerance and lead to increased DMS (Richier et al. 2018, Hopkins and Archer
738 2014). This supports the hypothesis that populations from higher latitude, less well-buffered
739 waters, already possess a certain degree of acclimative tolerance to variations in carbonate
740 chemistry environment. Although initial community size structure was not a significant
741 predictor of the response to high CO₂, it is possible that a combination of both community
742 composition and the natural range in variability in carbonate chemistry – as a function of
743 buffer capacity – may influence the DMS/P response to OA over a range of timescales
744 (Richier et al. 2018).

745 Our findings should be considered in the context of timescales of change (experimental vs
746 real world OA) and the potential of microbial communities to adapt to a gradually changing
747 environment. Microcosm experiments focus on the physiological response of microbial
748 communities to short term OA. Mesocosm experiments consider a timescale that allows the
749 response to be driven by community composition shifts, but are not long enough in duration
750 to incorporate an adaptive response. Neither approach is likely to accurately simulate the
751 response to the gradual changes in surface ocean pH that will occur over the next 50 – 100
752 years, nor the resulting changes in microbial community structure and distribution. However,

753 we hypothesise that the DMS response to OA should be considered not only in relation to
754 experimental perturbations to carbonate chemistry, but also in relation to the magnitude of
755 background variability in carbonate chemistry experienced by the DMS-producing organisms
756 and communities. Our findings suggest a strong link between the DMS response to OA and
757 background regional variability in the carbonate chemistry.

758 Models suggest the climate may be sensitive to changes in the spatial distribution of DMS
759 emissions over global scales (Woodhouse et al., 2013; Menzo et al., 2018). Such changes
760 could be driven by both physiological and adaptive responses to environmental change.

761 Accepting the limitations of experimental approaches, our findings suggest that net DMS
762 production from polar oceans may be resilient to OA in the context of its short term effects
763 on microbial communities. The oceans face a multitude of CO₂-driven changes in the coming
764 decades, including OA, warming, deoxygenation and loss of sea ice (Gattuso et al., 2015).
765 Our study addresses only one aspect of these future ocean stressors, but contributes to our
766 understanding of how DMS emissions from the polar oceans may alter, facilitating a better
767 understanding of Earth's future climate.

768 **Data availability**

769 All data has been deposited in and is accessible from the British Oceanographic Data Centre.

770 **Author contributions**

771 CMM, SR, FH, PDN and SDA designed the experiments. FH and JAS conducted the
772 measurements, FH and GLC analysed the data. FH prepared the paper with assistance and
773 contributions from all co-authors.

774 **Competing interests**

775 The authors declare that they have no conflict of interest.

776 **Financial support**

777 This work was funded under the UK Ocean Acidification thematic programme (UKOA) via
778 the UK Natural Environment Research Council (NERC) grants to PD Nightingale and SD
779 Archer (NE/H017259/1) and to T Tyrell, EP Achterberg and CM Moore (NE/H017348/1).
780 The UK Department for Environment, Food and Rural Affairs (Defra) and the UK
781 Department of Energy and Climate Change (DECC) also contributed to funding UKOA. The
782 National Science Foundation, United States, provided additional support to SD Archer ((NSF
783 OCE-1316133).

784 **Review statement**

785 This paper was edited by Gerhard Herdl and reviewed by three anonymous referees.

786 **Acknowledgements**

787 Our work and transit in the coastal waters of Greenland, Iceland and Svalbard was granted
788 thanks to permissions provided by the Danish, Icelandic and Norwegian diplomatic
789 authorities. We thank the captains and crew of the RRS Discovery (cruise D366) and RRS
790 James Clark Ross (cruises JR271 and JR274), and the technical staff of the National Marine
791 Facilities and the British Antarctic Survey. We are grateful to Mariana Ribas-Ribas and
792 Eithne Tynan for carbonate chemistry data, Elaine Mitchell and Clement Georges for flow
793 cytometry data, and Mariana Ribas-Ribas and Rob Thomas (BODC) for data management.

794 **References**

795 Archer, S. D., Kimmance, S. A., Stephens, J. A., Hopkins, F. E., Bellerby, R. G. J., Schulz,
796 K. G., Piontek, J., and Engel, A.: Contrasting responses of DMS and DMSP to ocean
797 acidification in Arctic waters, *Biogeosciences*, 10, 1893-1908, 10.5194/bg-10-1893-2013,
798 2013.
799

800 Avgoustidi, V., Nightingale, P. D., Joint, I. R., Steinke, M., Turner, S. M., Hopkins, F. E.,
801 and Liss, P. S.: Decreased marine dimethyl sulfide production under elevated CO₂ levels in
802 mesocosm and in vitro studies, *Environ. Chem.*, 9, 399-404, 2012.

803
804 Bigg, E. K., and Leck, C.: Properties of the aerosol over the central Arctic Ocean, *Journal of*
805 *Geophysical Research: Atmospheres*, 106, 32101-32109, 2001.

806
807 Brussaard, C. P. D., Noordeloos, A. A. M., Witte, H., Collentour, M. C. J., Schulz, K.,
808 Ludwig, A., and Riebesell, U.: Arctic microbial community dynamics influenced by elevated
809 CO₂ levels, *Biogeosciences*, 10, 719-731, 10.5194/bg-10-719-2013, 2013.

810
811 Carpenter, L. J., Archer, S. D., and Beale, R.: Ocean-atmosphere trace gas exchange,
812 *Chemical Society Reviews*, 41, 6473-6506, 2012.

813
814 Chang, R. Y. W., Sjostedt, S. J., Pierce, J. R., Papakyriakou, T. N., Scarratt, M. G., Michaud,
815 S., Levasseur, M., Leaitch, W. R., and Abbatt, J. P.: Relating atmospheric and oceanic DMS
816 levels to particle nucleation events in the Canadian Arctic, *Journal of Geophysical Research:*
817 *Atmospheres*, 116, 2011.

818
819 Charlson, R. J., Lovelock, J. E., Andreae, M. O., and Warren, S. G.: Oceanic phytoplankton,
820 atmospheric sulphur, cloud albedo and climate, *Nature*, 326, 655-661, 1987.

821
822 Chen, T., and Jang, M.: Secondary organic aerosol formation from photooxidation of a
823 mixture of dimethyl sulfide and isoprene, *Atmospheric Environment*, 46, 271-278, 2012.

824
825 Coello-Camba, A., Agustí, S., Holding, J., Arrieta, J. M., and Duarte, C. M.: Interactive effect
826 of temperature and CO₂ increase in Arctic phytoplankton, *Frontiers in Marine Science*, 1, 49,
827 2014.

828
829 Crawford, K. J., Brussaard, C. P. D., and Riebesell, U.: Shifts in the microbial community in
830 the Baltic Sea with increasing CO₂, *Biogeosciences Discuss.*, 2016, 1-51, 10.5194/bg-2015-
831 606, 2016.

832
833 Davidson, A. T., McKinlay, J., Westwood, K., Thompson, P., van den Enden, R., de Salas,
834 M., Wright, S., Johnson, R., and Berry, K.: Enhanced CO₂ concentrations change the
835 structure of Antarctic marine microbial communities, *Mar Ecol Prog Ser.* doi, 10, 3354, 2016.

836
837 del Valle, D. A., Kieber, D. J., Toole, D. A., Bisgrove, J., and Kiene, R. P.: Dissolved DMSO
838 production via biological and photochemical oxidation of dissolved DMS in the Ross Sea,
839 Antarctica, *Deep Sea Research Part I: Oceanographic Research Papers*, 56, 166-177,
840 <http://dx.doi.org/10.1016/j.dsr.2008.09.005>, 2009.

841
842 Egleston, E. S., Sabine, C. L., and Morel, F. M. M.: Revelle revisited: Buffer factors that
843 quantify the response of ocean chemistry to changes in DIC and alkalinity, *Global*
844 *Biogeochemical Cycles*, 24, n/a-n/a, 10.1029/2008gb003407, 2010.

845
846 Engel, A., Zondervan, I., Aerts, K., Beaufort, L., Benthien, A., Chou, L., Delille, B., Gattuso,
847 J.-P., Harlay, J., Heeman, C., Hoffman, L., Jacquet, S., Nejstgaard, J., Pizay, M.-D.,
848 Rochelle-Newall, E., Schneider, U., Terbrueggen, A., and Riebesell, U.: Testing the direct

849 effect of CO₂ concentrations on a bloom of the coccolithophorid *Emiliania huxleyi* in
850 mesocosm experiments, *Limnology and Oceanography*, 50, 493-507, 2005.

851

852 Engel, A., Schulz, K., Riebesell, U., Bellerby, R., Delille, B., and Schartau, M.: Effects of
853 CO₂ on particle size distribution and phytoplankton abundance during a mesocosm bloom
854 experiment (PeECE II), *Biogeosciences*, 5, 509-521, 2008.

855

856 Eppley, R. W.: Temperature and phytoplankton growth in the sea, *Fish. bull.*, 70, 1063-1085,
857 1972.

858

859 Fassbender, A. J., Sabine, C. L., and Feifel, K. M.: Consideration of coastal carbonate
860 chemistry in understanding biological calcification, *Geophysical Research Letters*, 43, 4467-
861 4476, 10.1002/2016gl068860, 2016.

862

863 Flynn, K. J., Blackford, J. C., Baird, M. E., Raven, J. A., Clark, D. R., Beardall, J., Brownlee,
864 C., Fabian, H., and Wheeler, G. L.: Changes in pH at the exterior surface of plankton with
865 ocean acidification, *Nature Climate Change*, 2, 510-513, 2012.

866

867 Gabric, A. J., Qu, B., Matrai, P. A., Murphy, C., Lu, H., Lin, D. R., Qian, F., and Zhao, M.:
868 Investigating the coupling between phytoplankton biomass, aerosol optical depth and sea-ice
869 cover in the Greenland Sea, *Dynamics of Atmospheres and Oceans*, 66, 94-109,
870 <http://dx.doi.org/10.1016/j.dynatmoce.2014.03.001>, 2014.

871

872 Galindo, V., Levasseur, M., Mundy, C. J., Gosselin, M., Scarratt, M., Papakyriakou, T.,
873 Stefels, J., Gale, M. A., Tremblay, J.-É., and Lizotte, M.: Contrasted sensitivity of DMSP
874 production to high light exposure in two Arctic under-ice blooms, *Journal of Experimental
875 Marine Biology and Ecology*, 475, 38-48, <http://dx.doi.org/10.1016/j.jembe.2015.11.009>,
876 2016.

877

878 Gattuso, J.-P., Lee, K., Rost, B., and Schulz, K.: Approaches and tools to manipulate the
879 carbonate chemistry, in: *Guide to Best Practices for Ocean Acidification Research and Data
880 Reporting*, edited by: Riebesell, U., Fabry, V. J., Hansson, L., and Gattuso, J. P.,
881 Publications Office of the European Union, Luxembourg, 263, 2010.

882

883 Gattuso, J.-P., Magnan, A., Bille, R., Cheung, W., Howes, E., Joos, F., Allemand, D., Bopp,
884 L., Cooley, S., and Eakin, C.: Contrasting futures for ocean and society from different
885 anthropogenic CO₂ emissions scenarios, *Science*, 349, aac4722, 2015.

886

887 Hagens, M., and Middelburg, J. J.: Attributing seasonal pH variability in surface ocean
888 waters to governing factors, *Geophysical Research Letters*, 43, 12,528-512,537,
889 doi:10.1002/2016GL071719, 2016.

890

891 Hauri, C., Friedrich, T., and Timmermann, A.: Abrupt onset and prolongation of aragonite
892 undersaturation events in the Southern Ocean, *Nature Clim. Change*, 6, 172-176,
893 10.1038/nclimate2844

894 [http://www.nature.com/nclimate/journal/v6/n2/abs/nclimate2844.html#supplementary-](http://www.nature.com/nclimate/journal/v6/n2/abs/nclimate2844.html#supplementary-information)
895 [information](http://www.nature.com/nclimate/journal/v6/n2/abs/nclimate2844.html#supplementary-information), 2016.

896

897 Holding, J. M., Duarte, C. M., Sanz-Martin, M., Mesa, E., Arrieta, J. M., Chierici, M.,
898 Hendriks, I. E., Garcia-Corral, L. S., Regaudie-de-Gioux, A., Delgado, A., Reigstad, M.,
899 Wassmann, P., and Agusti, S.: Temperature dependence of CO₂-enhanced primary
900 production in the European Arctic Ocean, *Nature Climate Change*, 5, 1079,
901 10.1038/nclimate2768, 2015.

902
903 Hönlisch, B., Ridgwell, A., Schmidt, D. N., Thomas, E., Gibbs, S. J., Sluijs, A., Zeebe, R.,
904 Kump, L., Martindale, R. C., Greene, S. E., Kiessling, W., Ries, J., Zachos, J. C., Royer, D.
905 L., Barker, S., Marchitto, T. M., Moyer, R., Pelejero, C., Ziveri, P., Foster, G. L., and
906 Williams, B.: The Geological Record of Ocean Acidification, *Science*, 335, 1058-1063,
907 10.1126/science.1208277, 2012.

908
909 Hopkins, F. E., Turner, S. M., Nightingale, P. D., Steinke, M., Bakker, D., and Liss, P. S.:
910 Ocean acidification and marine trace gas emissions, *Proceedings of the National Academy of*
911 *Sciences*, 107, 760-765, 2010.

912
913 Hopkins, F. E., and Archer, S. D.: Consistent increase in dimethyl sulfide (DMS) in response
914 to high CO₂ in five shipboard bioassays from contrasting NW European waters,
915 *Biogeosciences*, 11, 4925-4940, 10.5194/bg-11-4925-2014, 2014.

916
917
918 Hoppe, C. J., Schuback, N., Semeniuk, D. M., Maldonado, M. T., and Rost, B.: Functional
919 Redundancy Facilitates Resilience of Subarctic Phytoplankton Assemblages toward Ocean
920 Acidification and High Irradiance, *Frontiers in Marine Science*, 4, 229, 2017.

921
922 Hoppe, C. J. M., Hassler, C. S., Payne, C. D., Tortell, P. D., Rost, B., and Trimborn, S.: Iron
923 Limitation Modulates Ocean Acidification Effects on Southern Ocean Phytoplankton
924 Communities, *PLOS ONE*, 8, e79890, 10.1371/journal.pone.0079890, 2013.

925
926 Hoppe, C. J. M., Wolf, K. K. E., Schuback, N., Tortell, P. D., and Rost, B.: Compensation of
927 ocean acidification effects in Arctic phytoplankton assemblages, *Nature Climate Change*, 8,
928 529-533, 10.1038/s41558-018-0142-9, 2018.

929
930 Husherr, R., Levasseur, M., Lizotte, M., Tremblay, J.-É., Mol, J., Helmuth, T., Gosselin, M.,
931 Starr, M., Miller, L. A., and Jarníková, T.: Impact of ocean acidification on Arctic
932 phytoplankton blooms and dimethyl sulfide concentration under simulated ice-free and
933 under-ice conditions, *Biogeosciences*, 14, 2407, 2017.

934
935 Jarníková, T., and Tortell, P. D.: Towards a revised climatology of summertime
936 dimethylsulfide concentrations and sea-air fluxes in the Southern Ocean, *Environ. Chem.*, 13,
937 364-378, <http://dx.doi.org/10.1071/EN14272>, 2016.

938
939 Johnson, M. T., and Bell, T. G.: Coupling between dimethylsulfide emissions and the ocean-
940 atmosphere exchange of ammonia, *Environ. Chem.*, 5, 259-267, doi:10.1071/EN08030, 2008.

941
942 Kapsenberg, L., Kelley, A. L., Shaw, E. C., Martz, T. R., and Hofmann, G. E.: Near-shore
943 Antarctic pH variability has implications for the design of ocean acidification experiments,
944 *Scientific Reports*, 5, 9638, 10.1038/srep09638, 2015.

945

946 Kiene, R. P., and Slezak, D.: Low dissolved DMSP concentrations in seawater revealed by
947 small-volume gravity filtration and dialysis sampling *Limnology and Oceanography*
948 *Methods*, 4, 80-95, 2006.

949

950 Kim, J. M., Lee, K., Shin, K., Kang, J. H., Lee, H. W., Kim, M., Jang, P. G., and Jang, M. C.:
951 The effect of seawater CO₂ concentration on growth of a natural phytoplankton assemblage
952 in a controlled mesocosm experiment, *Limnology and Oceanography*, 51, 1629-1636, 2006.

953

954 Kim, J. M., Lee, K., Yang, E. J., Shin, K., Noh, J. H., Park, K. T., Hyun, B., Jeong, H. J.,
955 Kim, J. H., Kim, K. Y., Kim, M., Kim, H. C., Jang, P. G., and Jang, M. C.: Enhanced
956 Production of Oceanic Dimethylsulfide Resulting from CO₂-Induced Grazing Activity in a
957 High CO₂ World, *Environmental Science & Technology*, 44, 8140-8143,
958 10.1021/es102028k, 2010.

959

960 Kitidis, V., Hardman-Mountford, N. J., Litt, E., Brown, I., Cummings, D., Hartman, S.,
961 Hydes, D., Fishwick, J. R., Harris, C., and Martinez-Vicente, V.: Seasonal dynamics of the
962 carbonate system in the Western English Channel, *Continental Shelf Research*, 42, 30-40,
963 2012.

964

965 Korhonen, H., Carslaw, K. S., Spracklen, D. V., Mann, G. W., and Woodhouse, M. T.:
966 Influence of oceanic dimethyl sulfide emissions on cloud condensation nuclei concentrations
967 and seasonality over the remote Southern Hemisphere oceans: A global model study, *Journal*
968 *of Geophysical Research-Atmospheres*, 113, 16, D1520410.1029/2007jd009718, 2008a.

969

970 Korhonen, H., Carslaw, K. S., Spracklen, D. V., Ridley, D. A., and Ström, J.: A global model
971 study of processes controlling aerosol size distributions in the Arctic spring and summer,
972 *Journal of Geophysical Research*, 113, D08211, 2008b.

973

974 Lana, A., Bell, T. G., Simó, R., Vallina, S. M., Ballabrera-Poy, J., Kettle, A. J., Dachs, J.,
975 Bopp, L., Saltzman, E. S., Stefels, J., Johnson, J. E., and Liss, P. S.: An updated climatology
976 of surface dimethylsulfide concentrations and emission fluxes in the global ocean, *Global*
977 *Biogeochem. Cycles*, 25, GB1004, 2011.

978

979 Leaitch, W. R., Sharma, S., Huang, L., Toom-Sauntry, D., Chivulescu, A., Macdonald, A.
980 M., von Salzen, K., Pierce, J. R., Bertram, A. K., and Schroder, J. C.: Dimethyl sulfide
981 control of the clean summertime Arctic aerosol and cloud, *Elementa: Science of the*
982 *Anthropocene*, 1, 000017, 2013.

983

984 Leakey, R.: *Effect of Ocean Acidification on Arctic Surface Ocean Biology,*
985 *Biogeochemistry and Climate, British Oceanographic Data Centre, 2012.*

986 Levasseur, M.: Impact of Arctic meltdown on the microbial cycling of sulphur, *Nature*
987 *Geoscience*, 6, 691-700, 2013.

988

989 Lewis, E., and Wallace, D. W. R.: *Program Developed for CO₂ System Calculations, Carbon*
990 *Dioxide Information Analysis Center, Oak Ridge National Laboratory, U.S. Department of*
991 *Energy, Oak Ridge, Tennessee., 1998.*

992

993 McCoy, D. T., Burrows, S. M., Wood, R., Grosvenor, D. P., Elliott, S. M., Ma, P.-L., Rasch,
994 P. J., and Hartmann, D. L.: Natural aerosols explain seasonal and spatial patterns of Southern
995 Ocean cloud albedo, *Science Advances*, 1, 10.1126/sciadv.1500157, 2015.

996
997 McNeil, B. I., and Matear, R. J.: Southern Ocean acidification: A tipping point at 450-ppm
998 atmospheric CO₂, *Proceedings of the National Academy of Sciences*, 105, 18860-18864,
999 2008.

1000
1001 Menzo, Z., Elliott, S., Hartin, C., Hoffman, F., and Wang, S.: Climate change impacts on
1002 natural sulfur production: Ocean acidification and community shifts, *Atmosphere*, 9, 167,
1003 2018.

1004
1005 Monier, A., Findlay, H. S., Charvet, S., and Lovejoy, C.: Late winter under ice pelagic
1006 microbial communities in the high Arctic Ocean and the impact of short-term exposure to
1007 elevated CO₂ levels, *Name: Frontiers in Microbiology*, 5, 490, 2014.

1008
1009 Orr, J. C., Fabry, V. J., Aumont, O., Bopp, L., Doney, S. C., Feely, R. A., Gnanadesikan, A.,
1010 Gruber, N., Ishida, A., and Joos, F.: Anthropogenic ocean acidification over the twenty-first
1011 century and its impact on calcifying organisms, *Nature*, 437, 681-686, 2005.

1012
1013 Park, K.-T., Lee, K., Shin, K., Yang, E. J., Hyun, B., Kim, J.-M., Noh, J. H., Kim, M., Kong,
1014 B., Choi, D. H., Choi, S.-J., Jang, P.-G., and Jeong, H. J.: Direct Linkage between Dimethyl
1015 Sulfide Production and Microzooplankton Grazing, Resulting from Prey Composition
1016 Change under High Partial Pressure of Carbon Dioxide Conditions, *Environmental Science &
1017 Technology*, 48, 4750-4756, 10.1021/es403351h, 2014.

1018
1019 Poulton, A. J., Daniels, C. J., Esposito, M., Humphreys, M. P., Mitchell, E., Ribas-Ribas, M.,
1020 Russell, B. C., Stinchcombe, M. C., Tynan, E., and Richier, S.: Production of dissolved
1021 organic carbon by Arctic plankton communities: Responses to elevated carbon dioxide and
1022 the availability of light and nutrients, *Deep Sea Research Part II: Topical Studies in
1023 Oceanography*, 127, 60-74, <http://dx.doi.org/10.1016/j.dsr2.2016.01.002>, 2016.

1024
1025 Raven, J., Caldeira, K., Elderfield, H., Hoegh-Guldberg, O., Liss, P., Riebesell, U., Shepherd,
1026 J., Turley, C., and Watson, A.: Ocean acidification due to increasing atmospheric carbon
1027 dioxide, *The Royal Society, Policy Document 12/05*, London, 2005.

1028
1029 Rempillo, O., Seguin, A. M., Norman, A. L., Scarratt, M., Michaud, S., Chang, R., Sjostedt,
1030 S., Abbatt, J., Else, B., and Papakyriakou, T.: Dimethyl sulfide air-sea fluxes and biogenic
1031 sulfur as a source of new aerosols in the Arctic fall, *Journal of Geophysical Research:
1032 Atmospheres*, 116, 2011.

1033
1034 Revelle, R., and Suess, H. E.: Carbon Dioxide Exchange Between Atmosphere and Ocean
1035 and the Question of an Increase of Atmospheric CO₂ during the Past Decades, *Tellus A*, 9,
1036 1957.

1037
1038 Richier, S., Achterberg, E. P., Dumousseaud, C., Poulton, A. J., Suggett, D. J., Tyrrell, T.,
1039 Zubkov, M. V., and Moore, C. M.: Phytoplankton responses and associated carbon cycling
1040 during shipboard carbonate chemistry manipulation experiments conducted around Northwest
1041 European shelf seas, *Biogeosciences*, 11, 4733-4752, 10.5194/bg-11-4733-2014, 2014.

1042
1043 Richier, S., Achterberg, E. P., Humphreys, M. P., Poulton, A. J., Suggett, D. J., Tyrrell, T.,
1044 and Moore, C. M.: Geographical CO₂ sensitivity of phytoplankton correlates with ocean
1045 buffer capacity, *Global Change Biology*, doi:10.1111/gcb.14324, 2018.

1046
1047 Riebesell, U., Gattuso, J. P., Thingstad, T. F., and Middelburg, J. J.: Preface "Arctic ocean
1048 acidification: pelagic ecosystem and biogeochemical responses during a mesocosm study",
1049 Biogeosciences, 10, 5619-5626, 10.5194/bg-10-5619-2013, 2013.
1050
1051 Rysgaard, S., Glud, R. N., Lennert, K., Cooper, M., Halden, N., Leakey, R., Hawthorne, F.,
1052 and Barber, D.: Ikaite crystals in melting sea ice-implications for pCO₂ and pH levels in
1053 Arctic surface waters, *The Cryosphere*, 6, 901, 2012.
1054
1055 Sabine, C. L., Feely, R. A., Gruber, N., Key, R. M., Lee, K., Bullister, J. L., Wanninkhof, R.,
1056 Wong, C. S., Wallace, D. W. R., Tilbrook, B., Millero, F. J., Peng, T.-H., Kozyr, A., Ono, T.,
1057 and Rios, A. F.: The oceanic sink for anthropogenic CO₂, *Science*, 305, 367-371, 2004.
1058
1059 Schoemann, V., Becquevort, S., Stefels, J., Rousseau, V., and Lancelot, C.: Phaeocystis
1060 blooms in the global ocean and their controlling mechanisms: a review, *Journal of Sea
1061 Research*, 53, 43-66, 2005.
1062
1063 Schulz, K. G., Riebesell, U., Bellerby, R. G. J., Biswas, H., Meyerhofer, M., Muller, M. N.,
1064 Egge, J. K., Nejstgaard, J. C., Neill, C., Wohlers, J., and Zollner, E.: Build-up and decline of
1065 organic matter during PeECE III, *Biogeosciences*, 5, 707-718, 2008.
1066
1067 Schulz, K. G., Bellerby, R. G. J., Brussaard, C. P. D., Büdenbender, J., Czerny, J., Engel, A.,
1068 Fischer, M., Koch-Klavsen, S., Krug, S. A., Lischka, S., Ludwig, A., Meyerhöfer, M.,
1069 Nondal, G., Silyakova, A., Stuhr, A., and Riebesell, U.: Temporal biomass dynamics of an
1070 Arctic plankton bloom in response to increasing levels of atmospheric carbon dioxide,
1071 *Biogeosciences*, 10, 161-180, 10.5194/bg-10-161-2013, 2013.
1072
1073 Schwinger, J., Tjiputra, J., Goris, N., Six, K. D., Kirkevåg, A., Seland, Ø., Heinze, C., and
1074 Ilyina, T.: Amplification of global warming through pH-dependence of DMS-production
1075 simulated with a fully coupled Earth system model (under review in *Biogeosciences*, doi:
1076 10.5194/bg-2017-33), *Biogeosciences*, 2017.
1077
1078 Sharma, S., Chan, E., Ishizawa, M., Toom-Sauntry, D., Gong, S., Li, S., Tarasick, D.,
1079 Leaitch, W., Norman, A., and Quinn, P.: Influence of transport and ocean ice extent on
1080 biogenic aerosol sulfur in the Arctic atmosphere, *Journal of Geophysical Research:
1081 Atmospheres*, 117, 2012.
1082
1083 Six, K. D., Kloster, S., Ilyina, T., Archer, S. D., Zhang, K., and Maier-Reimer, E.: Global
1084 warming amplified by reduced sulphur fluxes as a result of ocean acidification, *Nature
1085 Climate Change*, 3, 975, 2013.
1086
1087 Stefels, J.: Physiological aspects of the production and conversion of DMSP in marine algae
1088 and higher plants, *Journal of Sea Research*, 43, 183-197, 2000.
1089
1090 Steinacher, M., Joos, F., Frolicher, T. L., Plattner, G. K., and Doney, S. C.: Imminent ocean
1091 acidification in the Arctic projected with the NCAR global coupled carbon cycle-climate
1092 model, *Biogeosciences*, 6, 515-533, 2009.
1093
1094 Stillman, J. H., and Paganini, A. W.: Biochemical adaptation to ocean acidification, *Journal
1095 of Experimental Biology*, 218, 1946-1955, 10.1242/jeb.115584, 2015.

1096
1097 Sunda, W., Kieber, D. J., Kiene, R. P., and Huntsman, S.: An antioxidant function for DMSP
1098 and DMS in marine algae, *Nature*, 418, 317-320, 2002.
1099
1100 Tarling, G.: Sea Surface Ocean Acidification Consortium Cruise to the Southern Ocean,
1101 British Oceanographic Data Centre, 2013.
1102
1103 Thoisen, C., Riisgaard, K., Lundholm, N., Nielsen, T. G., and Hansen, P. J.: Effect of
1104 acidification on an Arctic phytoplankton community from Disko Bay, West Greenland,
1105 *Marine Ecology Progress Series*, 520, 21-34, 2015.
1106
1107 Thomas, D. N., and Dieckmann, G. S.: Antarctic Sea Ice--a Habitat for Extremophiles,
1108 *Science*, 295, 641-644, 10.1126/science.1063391, 2002.
1109
1110 Thomson, P. G., Davidson, A. T., and Maher, L.: Increasing CO₂ changes community
1111 composition of pico- and nano-sized protists and prokaryotes at a coastal Antarctic site,
1112 *Marine Ecology Progress Series*, 554, 51-69, 2016.
1113
1114 Tortell, P. D., Payne, C. D., Li, Y., Trimborn, S., Rost, B., Smith, W. O., Riesselman, C.,
1115 Dunbar, R. B., Sedwick, P., and DiTullio, G. R.: CO₂ sensitivity of Southern Ocean
1116 phytoplankton, *Geophysical Research Letters*, 35, 2008.
1117
1118 Trimborn, S., Brenneis, T., Hoppe, C. J. M., Laglera, L. M., Norman, L., Santos-Echeandía,
1119 J., Völkner, C., Wolf-Gladrow, D., and Hassler, C. S.: Iron sources alter the response of
1120 Southern Ocean phytoplankton to ocean acidification, *Marine Ecology Progress Series*, 578,
1121 35-50, 2017.
1122
1123 Tynan, E., Clarke, J. S., Humphreys, M. P., Ribas-Ribas, M., Esposito, M., Rérolle, V. M. C.,
1124 Schlosser, C., Thorpe, S. E., Tyrrell, T., and Achterberg, E. P.: Physical and biogeochemical
1125 controls on the variability in surface pH and calcium carbonate saturation states in the
1126 Atlantic sectors of the Arctic and Southern Oceans, *Deep Sea Research Part II: Topical
1127 Studies in Oceanography*, 127, 7-27, <http://dx.doi.org/10.1016/j.dsr2.2016.01.001>, 2016.
1128
1129 Vogt, M., Steinke, M., Turner, S., Paulino, A., Meyerhöfer, M., Riebesell, U., LeQuéré, C.,
1130 and Liss, P.: Dynamics of dimethylsulphoniopropionate and dimethylsulphide under different
1131 CO₂ concentrations during a mesocosm experiment, *Biogeosciences*, 5, 407-419, 2008.
1132
1133 von Glasow, R., and Crutzen, P. J.: Model study of multiphase DMS oxidation with a focus
1134 on halogens, *Atmos. Chem. Phys.*, 4, 589-608, 2004.
1135
1136 Webb, A. L., Malin, G., Hopkins, F. E., Ho, K. L., Riebesell, U., Schulz, K. G., Larsen, A.,
1137 and Liss, P. S.: Ocean acidification has different effects on the production of dimethylsulfide
1138 and dimethylsulfoniopropionate measured in cultures of *Emiliana huxleyi* and a mesocosm
1139 study: a comparison of laboratory monocultures and community interactions, *Environ.
1140 Chem.*, -, <http://dx.doi.org/10.1071/EN14268>, 2015.
1141
1142 Webb, A. L., Leedham-Elvidge, E., Hughes, C., Hopkins, F. E., Malin, G., Bach, L. T.,
1143 Schulz, K., Crawford, K., Brussaard, C. P. D., Stühr, A., Riebesell, U., and Liss, P. S.: Effect
1144 of ocean acidification and elevated fCO₂ on trace gas production by a Baltic Sea summer
1145 phytoplankton community, *Biogeosciences*, 13, 4595-4613, 10.5194/bg-13-4595-2016, 2016.

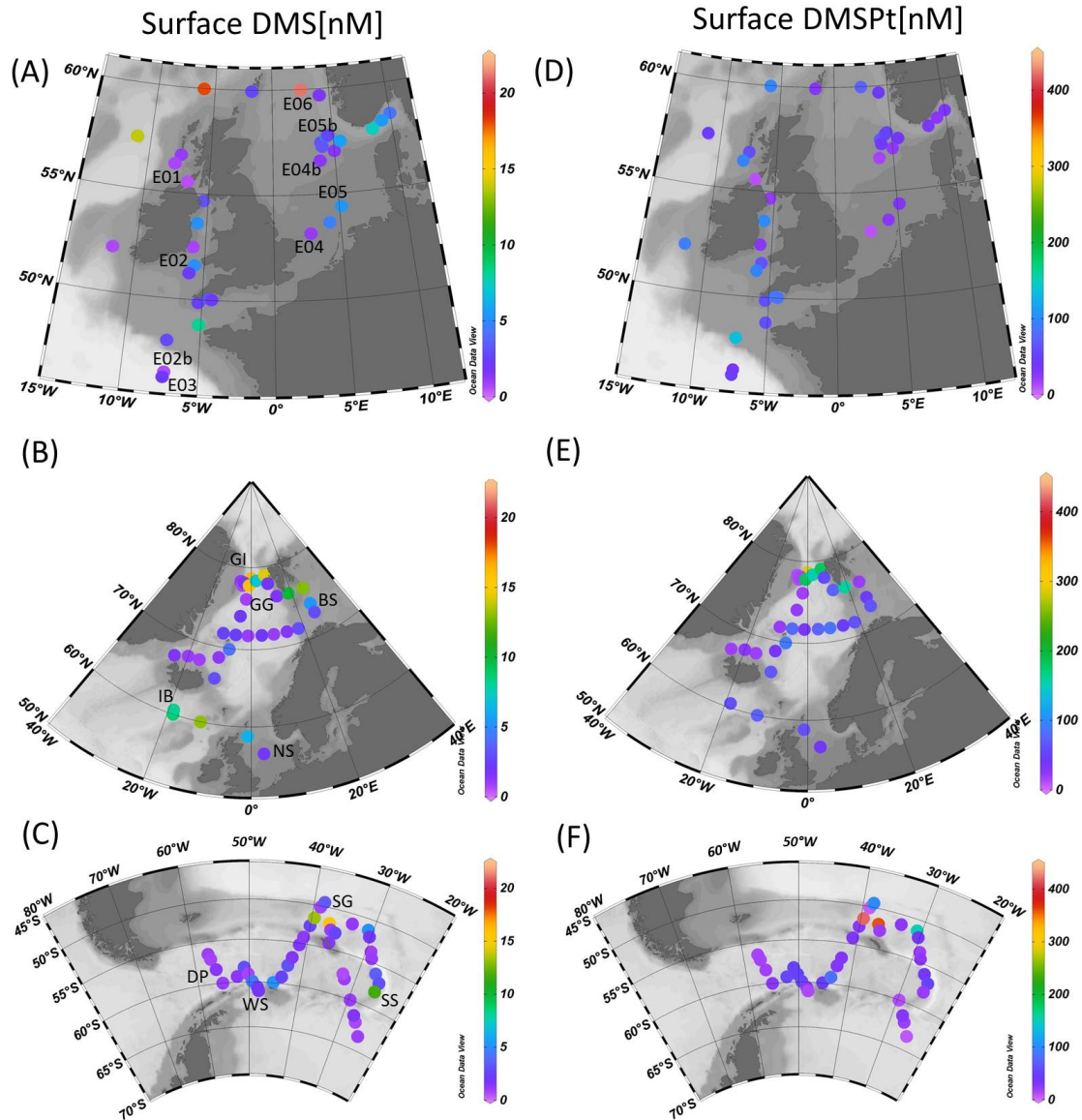
1146
1147 Woodhouse, M. T., Mann, G. W., Carslaw, K. S., and Boucher, O.: Sensitivity of cloud
1148 condensation nuclei to regional changes in dimethyl-sulphide emissions, *Atmos. Chem.*
1149 *Phys.*, 13, 2723-2733, 10.5194/acp-13-2723-2013, 2013.

1150 Table 1. Summary of the station locations and characteristic of the water sampled for the 18 microcosm experiments performed in temperate,
 1151 sub-polar and polar waters. All polar stations were sampled for JR271 and JR274, with the exception of NS and IB.

Cruise	Station ID	Location	Sampling location	Sampling date	Sampling depth (m)	SST (°C)	Salinity	Nitrate (uM)	Total Chl <i>a</i> ($\mu\text{g L}^{-1}$)	chl _{>10 μm} : chl _{total}	pCO ₂ (μatm) T ₀	pH (total) T ₀	Experimental timepoints T ₁ , T ₂ (hours)	Reference
D366	E01	Mingulay Reef	56°47.688N 7°24.300W	8 June 2011	6	11.3	34.8	1.1	3.3	no data	334.9	8.1	48, 96	<i>Hopkins & Archer (2011)</i>
	E02	Irish Sea	52°28.237N 5°54.052W	14 June 2011	5	11.8	34.4	0.3	3.5	0.80 ± 0.03	329.3	8.1	48, 96	<i>Hopkins & Archer (2011)</i>
	E02b	Bay of Biscay	46°29.794N 7°12.355W	19 June 2011	5	14.5	35.6	0.9	1.8	no data	340.3	8.1	48	<i>This study</i>
	E03	Bay of Biscay	46°12.137N 7°13.253W	21 June 2011	10	15.3	35.8	0.6	0.8	0.43 ± 0.03	323.9	8.1	48, 96	<i>Hopkins & Archer (2011)</i>
	E04	Southern North Sea	52°59.661N 2°29.841E	26 June 2011	5	14.6	34.1	0.9	1.3	0.19 ± 0.02	399.8	8.0	48, 96	<i>Hopkins & Archer (2011)</i>
	E04b	Mid North Sea	57°45.729N 4°35.434E	29 June 2011	5	13.2	34.8	No data	0.5	0.14 ± 0.003	327.3	8.1	48	<i>This study</i>
	E05	Mid North Sea	56°30.293N 3°39.506E	2 July 2011	12	14.0	35.0	0.2	0.3	0.23 ± 0.01	360.2	8.1	48, 96	<i>Hopkins & Archer (2011)</i>
	E05b	Atlantic Ocean	59°40.721N 4°07.633E	3 July 2011	4	13.4	30.7	0.3	0.7	0.12 ± 0.01	310.7	8.1	48	<i>This study</i>
	E06	Atlantic Ocean	59°59.011N 2°30.896E	3 July 2011	4	12.5	34.9	0.4	1.1	0.14 ± 0.01	287.1	8.2	48	<i>This study</i>
JR271	NS	Mid North Sea	56°15.59N 2°37.59E	3 June 2012	15	10.8	35.1	0.04	0.3	0.52 ± 0.05	300.5	8.2	48, 96	<i>This study</i>
	IB	Iceland Basin	60°35.39N 18°51.23W	8 June 2012	7	10.7	35.2	5.0	1.8	0.27 ± 0.02	309.7	8.1	48, 96	<i>This study</i>
	GG-AO	Greenland Gyre	76°10.52 N 2°32.96 W	13 June 2012	5	1.7	34.9	9.3	1.0	0.34 ± 0.001	289.3	8.2	48, 96	<i>This study</i>
	GI-AO	Greenland ice edge	78°21.15 N 3°39.85 W	18 June 2012	5	-1.6	32.6	4.2	2.7	0.78 ± 0.03	304.7	8.1	48, 96	<i>This study</i>
	BS-AO	Barents Sea	72°53.49 N 26°00.09 W	24 June 2012	5	6.6	35.0	5.4	1.3	0.04 ± 0.01	304.3	8.1	48, 96	<i>This study</i>
JR274	DP-SO	Drake Passage	58°22.00 S 56°15.12 W	13 Jan 2013	8	1.9	33.2	22.0	2.4	1.00 ± 0.06	279.3	8.2	48, 96	<i>This study</i>
	WS-SO	Weddell Sea	60°58.55 S 48°05.19 W	18 Jan 2013	6	-1.4	33.6	24.9	0.6	0.67 ± 0.06	510.5	7.9	72, 144	<i>This study</i>
	SG-SO	South Georgia	52°41.36 S 36°37.28 W	25 Jan 2013	5	2.2	33.9	24.1	0.7	0.35 ± 0.04	342.6	8.1	72, 144	<i>This study</i>
	SS-SO	South Sandwich	58°05.13 S 25°55.55 W	1 Feb 2013	7	0.5	33.7	18.5	4.6	0.57 ± 0.02	272.6	8.2	96, 168	<i>This study</i>

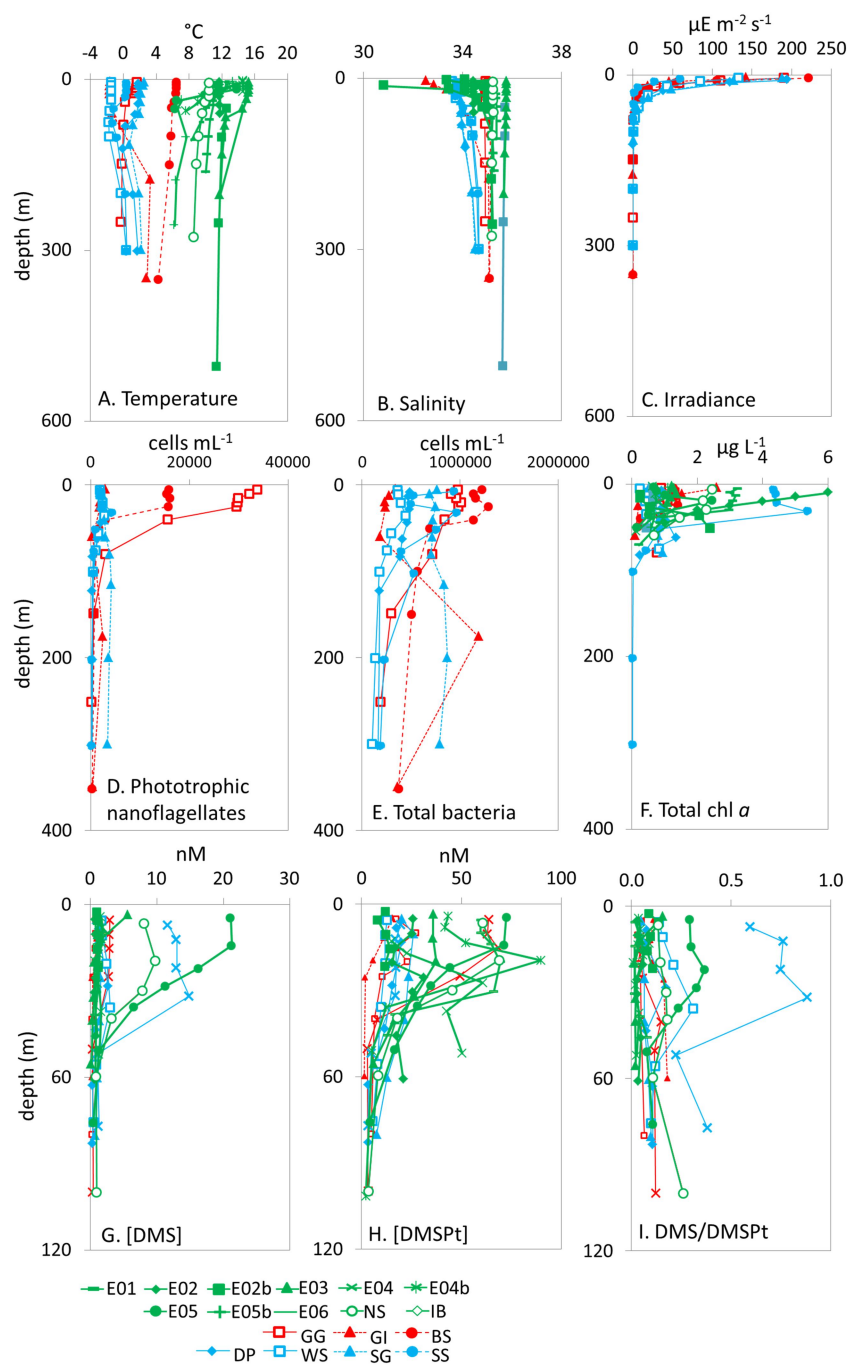
1152 Table 2. Mean (\pm SD) ratio of $>10\mu\text{m}$ Chl a to total Chl a ($\text{chl}_{>10\mu\text{m}}:\text{chl}_{\text{total}}$) for polar
 1153 microcosm sampling stations. * indicates significant difference from the response to ambient
 1154 CO_2 .

Station	Time	ambient	550 μatm	750 μatm	1000 μatm	2000 μatm
GG	48 h	0.3 ± 0.1	0.3 ± 0.03	0.4 ± 0.2	0.3 ± 0.1	N/A
	96 h	1.0 ± 0.02	0.9 ± 0.2	0.8 ± 0.1	0.7 ± 0.2	
GI	48 h	1.0 ± 0.1	1.0 ± 0.1	0.8 ± 0.1	1.0 ± 0.0	N/A
	96 h	1.0 ± 0.1	1.1 ± 0.1	0.8 ± 0.1	0.8 ± 0.1	
BS	48 h	0.02 ± 0.01	0.04 ± 0.01	0.03 ± 0.01	0.02 ± 0.01	N/A
	96 h	0.04 ± 0.01	0.05 ± 0.04	0.05 ± 0.04	0.04 ± 0.04	
DP	48 h	1.0 ± 0.3	N/A	1.0 ± 0.1	N/A	N/A
	96 h	0.9 ± 0.1		1.0 ± 0.1		
WS	72 h	0.6 ± 0.1	N/A	0.7 ± 0.1	N/A	N/A
	144 h	0.7 ± 0.1		0.7 ± 0.1		
SG	72 h	0.3 ± 0.02	N/A	0.4 ± 0.1	0.3 ± 0.1	0.4 ± 0.03
	144 h	0.5 ± 0.1		0.6 ± 0.04	0.5 ± 0.1	0.4 ± 0.03
SS	96 h	0.7 ± 0.04	N/A	$1.5 \pm 0.1^*$	0.7 ± 0.02	$1.6 \pm 0.1^*$
	168 h	0.9 ± 0.2		$1.4 \pm 0.02^*$	0.8 ± 0.004	$1.4 \pm 0.2^*$



1155

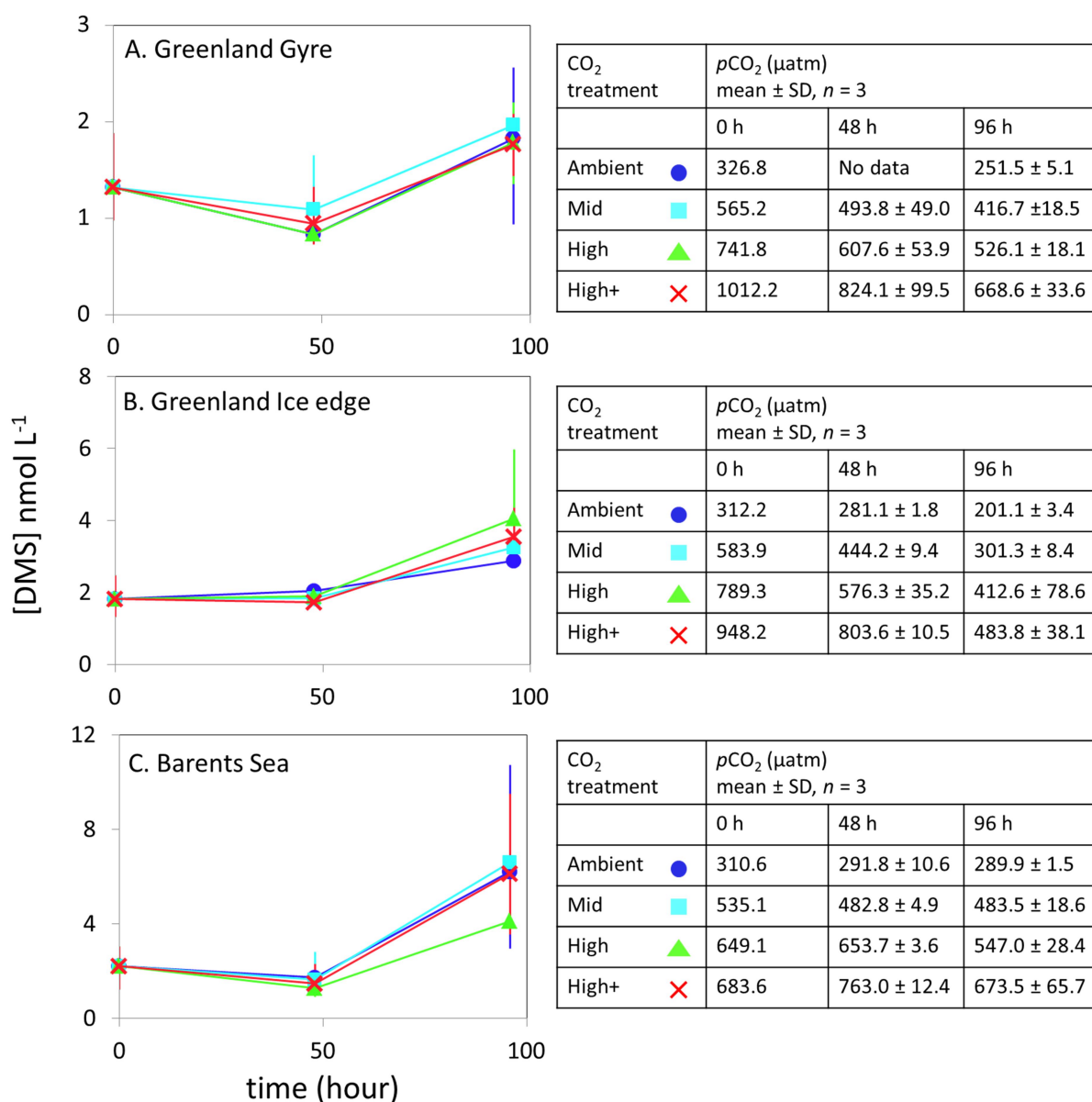
1156 Figure 1. Surface (<5 m) concentrations (nM) of DMS (A-C) and total DMSP (D-F) for
 1157 cruises in the NW European shelf (D366) (A,D), the sub-Arctic and Arctic Ocean (JR271)
 1158 (B,E) and the Southern Ocean (JR274) (C,F). Locations of sampling stations for microcosm
 1159 experiments shown in letters/numbers. E01 – E05: see Hopkins & Archer 2014. NS = *North*
 1160 *Sea*, IB = *Iceland Basin*, GI = *Greenland Ice-edge*, GG = *Greenland Gyre*, BS = *Barents Sea*,
 1161 DP = *Drake Passage*, WS = *Weddell Sea*, SG = *South Georgia*, SS = *South Sandwich*.



1162

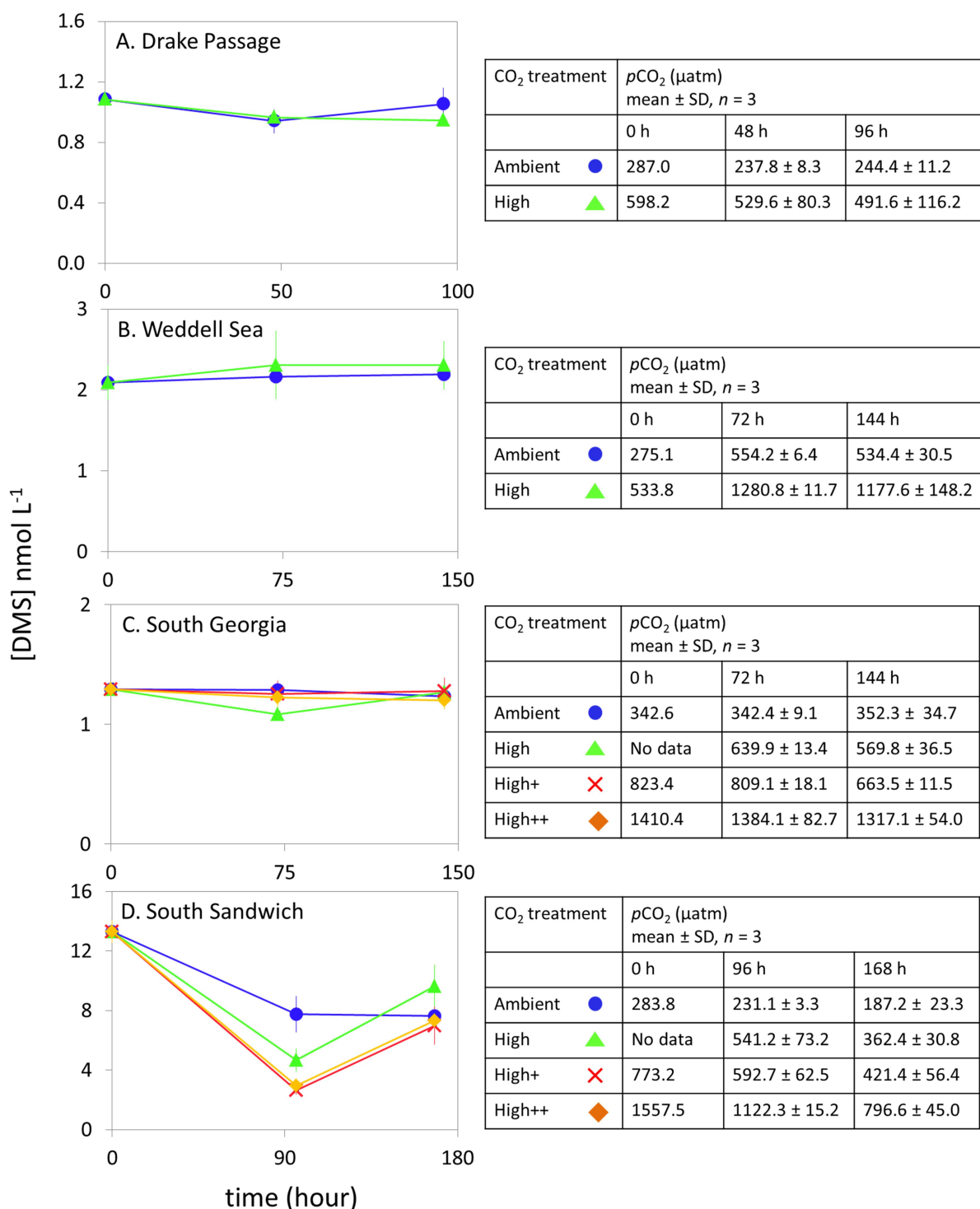
1163 Figure 2. Depth profiles for all 18 sampling stations showing A. Temperature (°C), B.
 1164 Salinity, C. Irradiance ($\mu\text{E m}^{-2} \text{s}^{-1}$), D. phototrophic nanoflagellate abundance (cells mL^{-1}), E.
 1165 total bacteria abundance (cells mL^{-1}), F. total Chl a ($\mu\text{g L}^{-1}$), G. [DMS] (nM), H. total
 1166 [DMSp] (nM) and I. DMS/DMSp from CTD casts at sampling stations for microcosm
 1167 experiments in temperate (green), Arctic (red) and Southern Ocean (blue) waters. See Table 1
 1168 for station details. Data for irradiance, phototrophic nanoflagellates and total bacteria were
 1169 not collected for temperate stations.

1170



1171

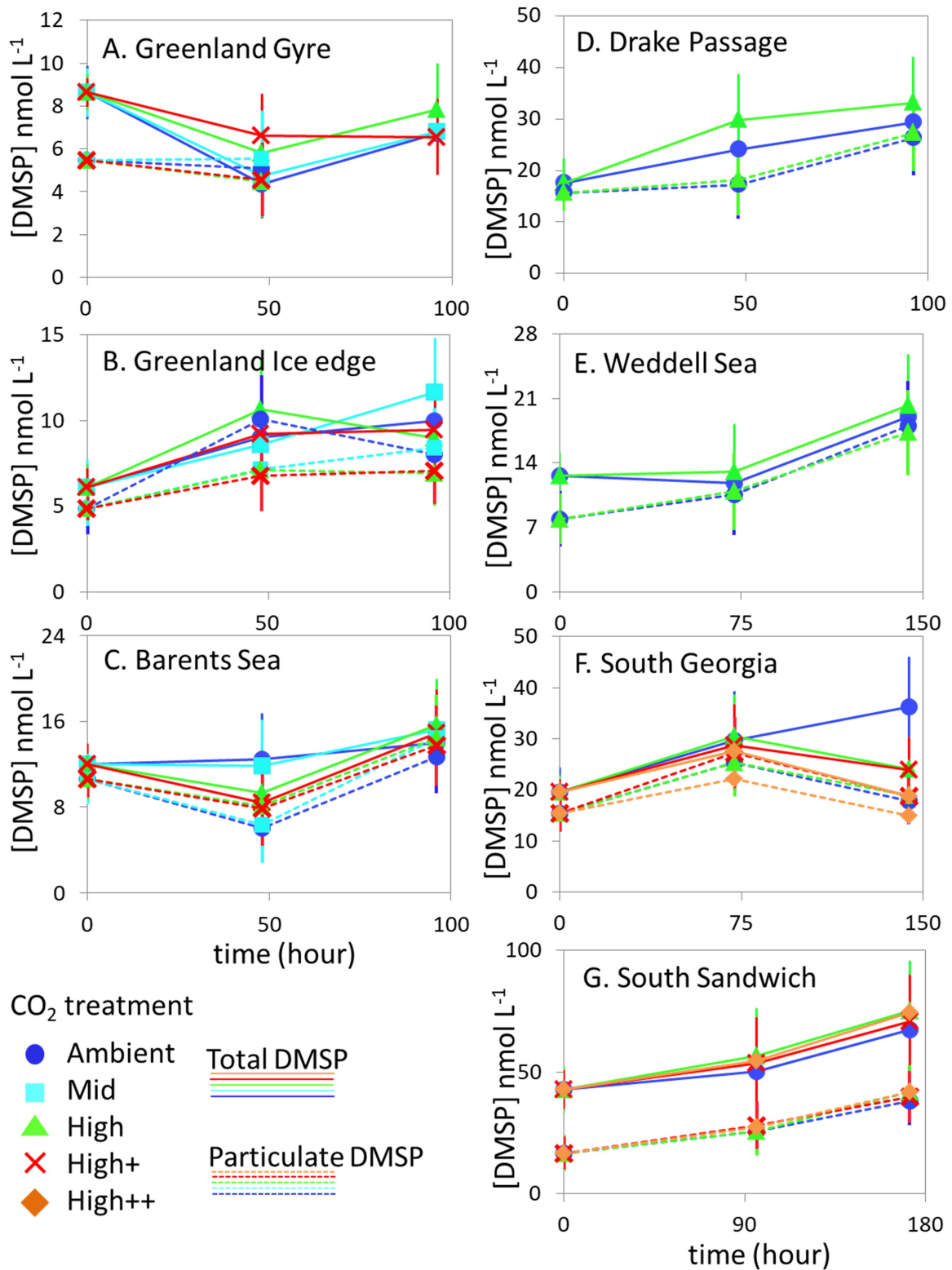
1172 Figure 3. DMS concentrations (nmol L⁻¹) during experimental microcosms performed in
 1173 Arctic waters. Data shown is mean of triplicate incubations, and error bars show standard
 1174 error on the mean. Tables show measurements of pCO₂ (μatm) for each treatment at each
 1175 sampling time point. Initial measurements (0 h) were from a single sample, whilst
 1176 measurements at 48 h and 96 h show mean ± SD of triplicate experimental bottles. Locations
 1177 of water collection for microcosms shown in Figure 1 C – F.



1178

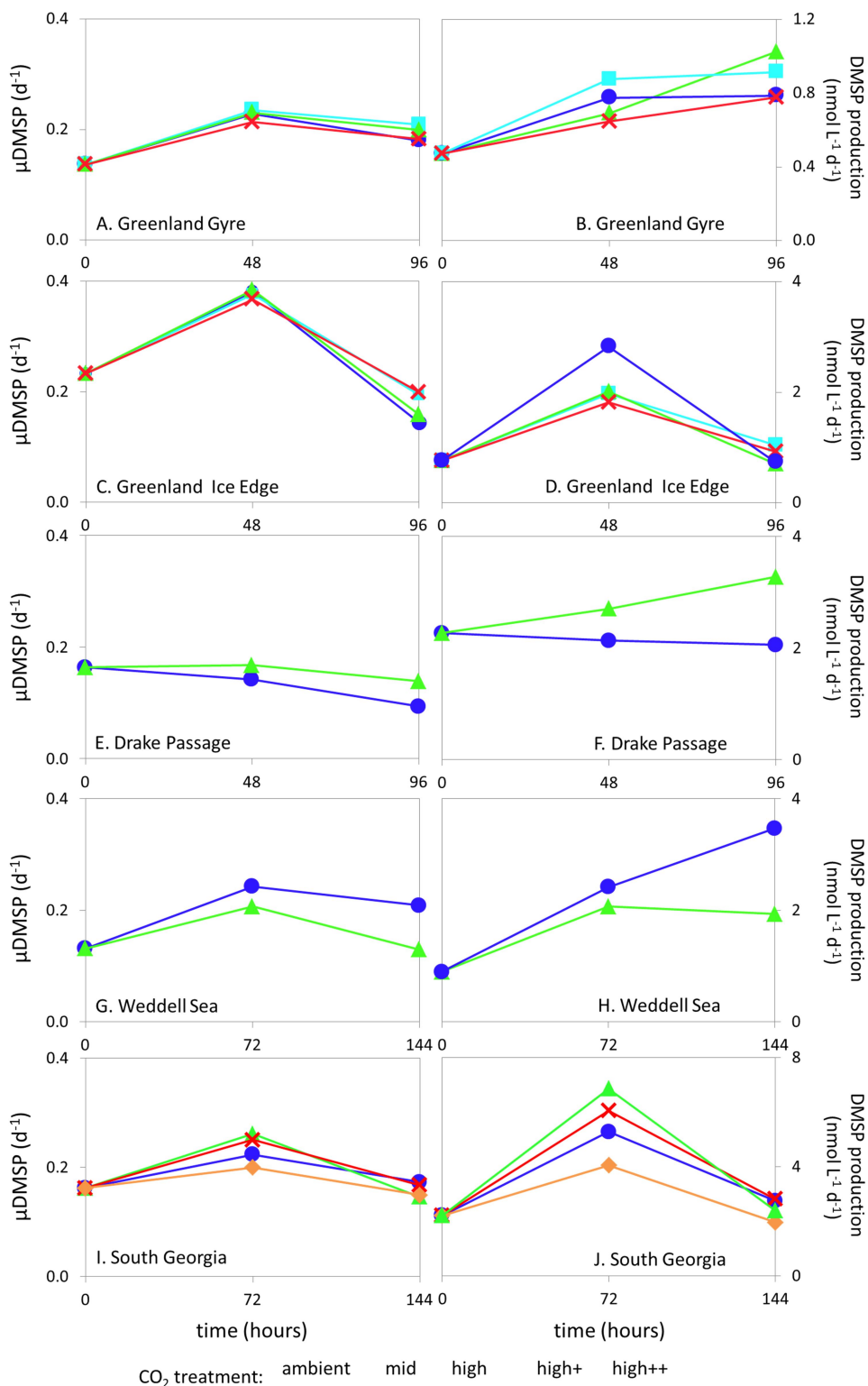
1179 Figure 4. DMS concentrations (nmol L⁻¹) during experimental microcosms performed in
 1180 Southern Ocean waters. Data shown is mean of triplicate incubations, and error bars show
 1181 standard error on the mean. Tables show measurements of pCO₂ (μatm) for each treatment at
 1182 each sampling time point. Initial measurements (0 h) were from a single sample, whilst
 1183 measurements at 48 h and 96 h show mean ± SD of triplicate experimental bottles. Locations
 1184 of water collection for microcosms shown in Figure 1 C – F.

1185



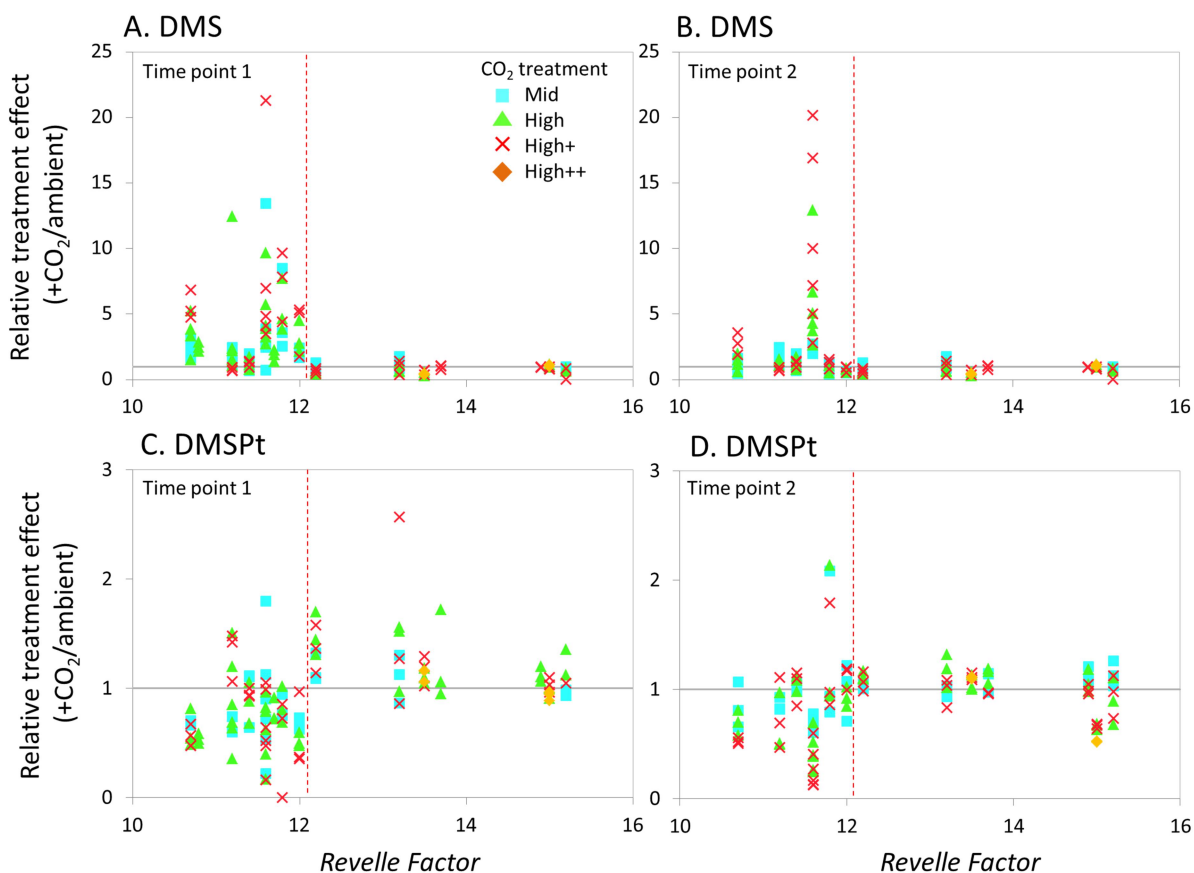
1186

1187 Figure 5. Total DMSP (solid lines) and particulate DMSP (dashed lines) concentrations (
 1188 nmol L⁻¹) during experimental microcosms performed in Arctic waters (A - C) and in
 1189 Southern Ocean waters (D - G). Data shown is mean of triplicate incubations, and error bars
 1190 show standard error on the mean. Locations of water collection for microcosms shown in
 1191 Figure 1 C - F. Particulate DMSP concentrations were used in calculations of DMSP
 1192 production rates (Figure 6).



1194
 1195 Figure 6. De novo synthesis of DMSP (μDMSP , d^{-1}) (left column) and DMSP production
 1196 rates ($\text{nmol L}^{-1} \text{d}^{-1}$) (right column) for Arctic Ocean stations *Greenland Gyre* (A,B),
 1197 *Greenland Ice-edge* (C, D) and Southern Ocean stations *Drake Passage* (E, F), *Weddell Sea*
 1198 (*G, H*) and *South Georgia* (I, J). No data is available for *Barents Sea* (Arctic Ocean) or *South*
 1199 *Sandwich* (Southern Ocean).

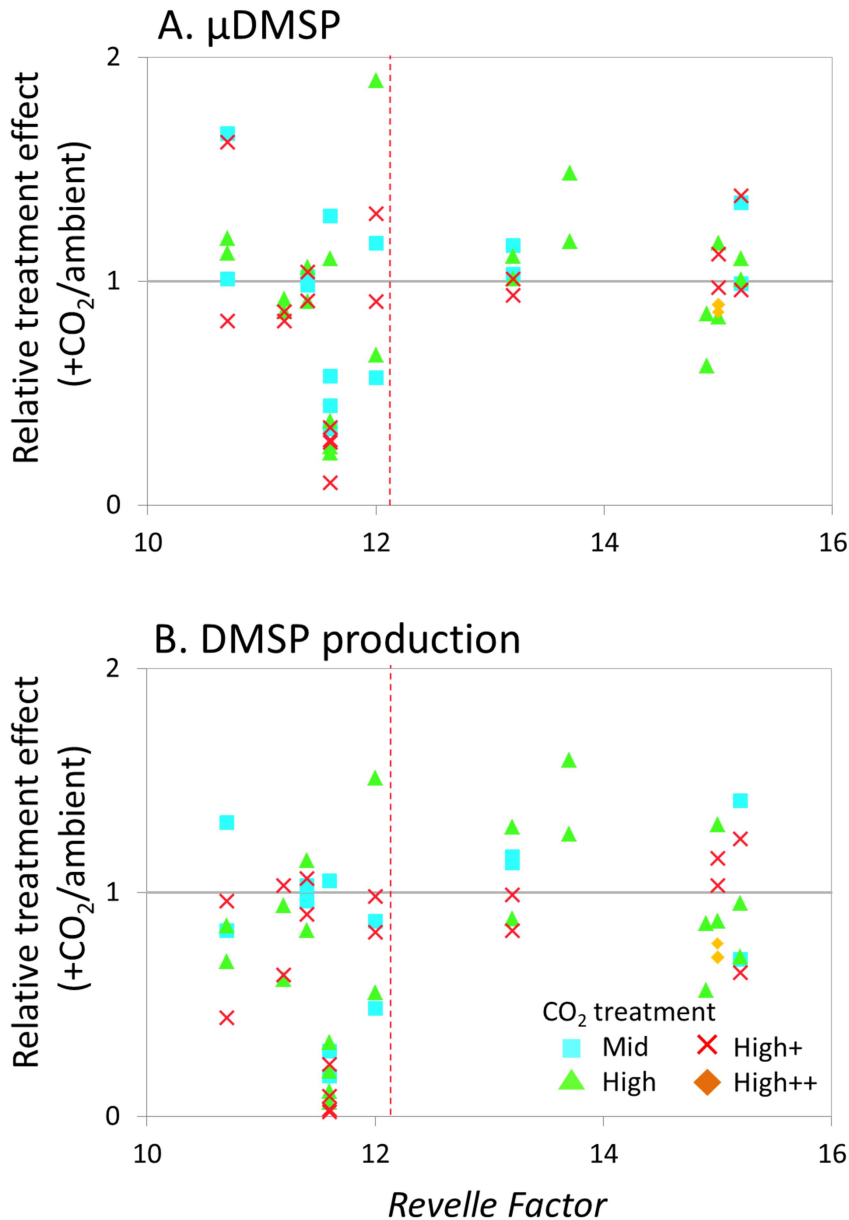
1200



1201

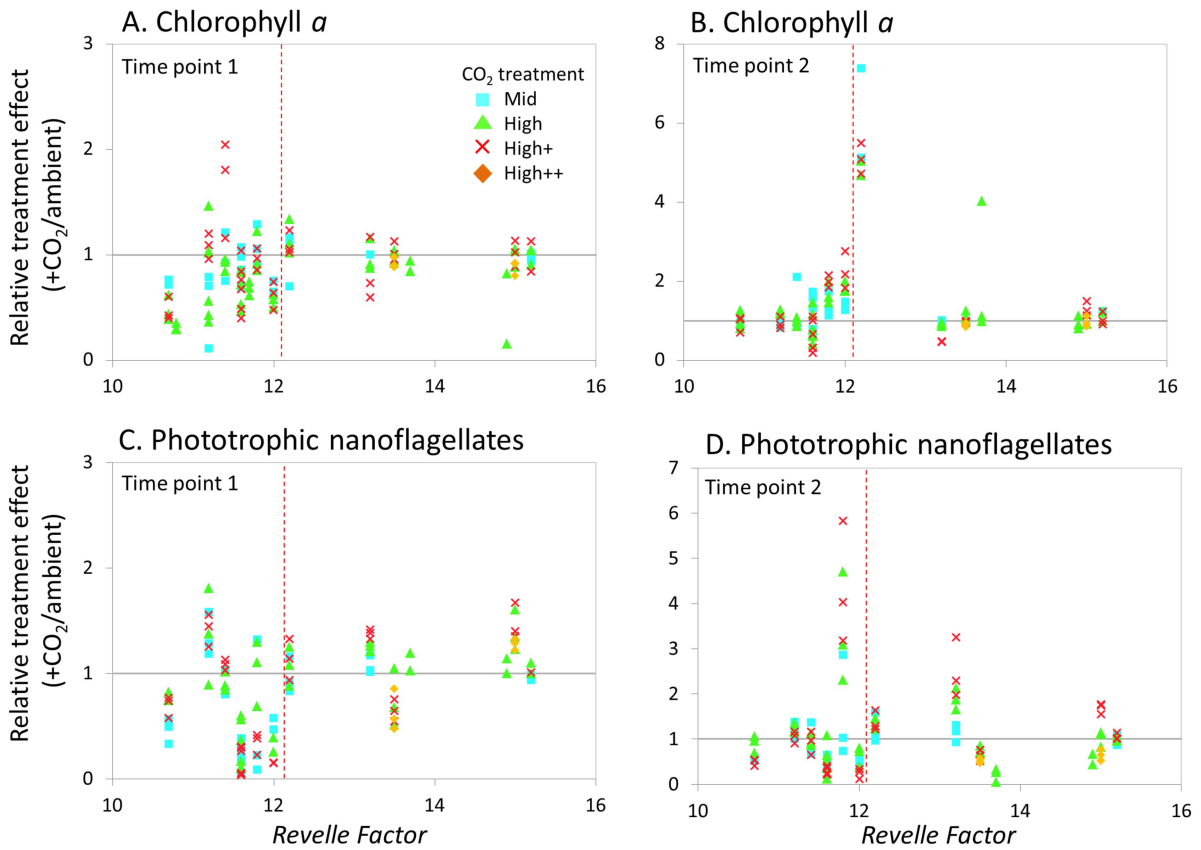
1202 Figure 7. Relationship between Revelle Factor of the sampled water and the relative CO₂
 1203 treatment effect at ($[x]_{\text{highCO}_2}/[x]_{\text{ambientCO}_2}$) for concentrations of DMS at T₁ (A) and T₂ (B),
 1204 and for total DMSPt concentrations at T₁ (C) and T₂ (D) for all microcosm experiments
 1205 performed in NW European waters, sub-Arctic and Arctic waters, and the Southern Ocean.
 1206 Grey solid line (= 1) indicates no effect of elevated CO₂. Revelle Factor > 12 = polar waters
 1207 (indicated by red dashed line). T₁ = 48 h, except for WS and SG (72 h) and SS (96 h). For
 1208 detailed analyses of the NW European shelf data, see Hopkins & Archer (2014).

1209



1210

1211 Figure 8. Relationship between the Revelle Factor of the sampled water and the relative CO₂
 1212 treatment effect at ($[x]_{\text{highCO}_2}/[x]_{\text{ambientCO}_2}$) for de novo DMSP synthesis (μDMSP , d^{-1}) at T₁
 1213 (A) and T₂ (B), and DMSP production rate ($\text{nmol L}^{-1} \text{d}^{-1}$) at T₁ (C) and T₂ (D) for microcosm
 1214 experiments performed in NW European waters, sub-Arctic and Arctic waters, and the
 1215 Southern Ocean. Grey solid line (= 1) indicates no effect of elevated CO₂. Revelle Factor >12
 1216 = polar waters (indicated by red dashed line). T₁ = 48 h, T₂ = 96 h, except for *Weddell Sea*
 1217 and *South Georgia* (72 h, 144 h). For discussion of the NW European shelf data, see Hopkins
 1218 & Archer (2014).



1219

1220 Figure 9. Relationship between the Revelle Factor of the sampled water and the relative CO₂
 1221 treatment effect ($[x]_{\text{highCO}_2}/[x]_{\text{ambientCO}_2}$) for chlorophyll *a* concentrations at T₁ (A) and T₂ (B)
 1222 and phototrophic nanoflagellate abundance at T₁ (C) and T₂ (D) for all microcosm
 1223 experiments performed in NW European waters, sub-Arctic and Arctic waters, and the
 1224 Southern Ocean. Grey solid line (= 1) indicates no effect of elevated CO₂. Revelle Factor >12
 1225 = polar waters (indicated by red dashed line). T₁ = 48 h, T₂ = 96 h, except for *Weddell Sea*
 1226 and *South Georgia* (72 h, 144 h) and *South Sandwich* (96 h, 168 h).

1227

1228